The maintenance of genetic polymorphism in sexually antagonistic traits

Ewan Flintham[1,2], Vincent Savolainen[2], Sarah Otto[3], Max Reuter[4] and Charles Mullon[1]

[1]Department of Ecology and Evolution, University of Lausanne, 1015 Lausanne, Switzerland

[2]Department of Life Sciences, Georgina Mace Centre for the Living Planet, Silwood Park Campus, Imperial College London, Ascot, SL5 7PY United Kingdom

[3]Department of Zoology, and Biodiversity Research Centre, University of British Columbia, Vancouver, British Columbia, Canada

[4]Department of Genetics, Evolution and Environment, University College London, London, WC1E 6BT United Kingdom

Abstract. Selection often favours different trait values in males and females, leading to genetic conflicts between the sexes, or sexual antagonism. Theory suggests that such conflict can maintain genetic variation by generating balancing selection. However, most of this theory is based on insights from models of single loci with fixed fitness effects. It is thus unclear how readily sexual antagonism drives balancing selection at loci where the fitness effects are not arbitrarily set but emerge from the genotype-phenotype map and the fitness landscape. Here we use mathematical models and computer simulations to investigate the evolution of traits that have different optima in males and females and so experience sexually antagonistic selection. We examine the consequences of such selection for the maintenance and nature of genetic variation under different assumptions of genetic architecture and for different fitness landscapes. We show that the conditions necessary to maintain variation are significantly more restrictive than previously appreciated. This is because the majority of typical sex-specific fitness landscapes generate stabilising selection on traits, and so favour the fixation of a single homozygote genotype that encodes the phenotype with the highest sex-averaged fitness. Instead, the maintenance of genetic polymorphism requires extremely, if not implausibly, strong conflict between males and females in order to disfavour extreme and intermediate phenotypes by generating diversifying selection. Furthermore, in all cases, we find that distinctive patterns of genetic variation produced by sexual antagonism arise rarely and are often transient, and so are difficult to observe in genomic data. Taken together, our results indicate that sex-specific selection is not a straightforward source of balanced genetic polymorphism and leaves few traces in the genome. Rather, we suggest that sexual antagonism is most likely to maintain genetic variation when traits are determined by a single large effect locus where genetic constraints lead to a limited range of possible alleles.

Keywords: Polymorphism, Balancing selection, Sexual conflict, Negative frequency dependence

1 Introduction

In sexual populations, intralocus genetic conflicts can arise between males and females when traits that are genetically correlated across the sexes have sex-specific phenotypic optima [1–3]. Here, selection acts in opposite directions in each sex, and as a result, alleles with similar phenotypic effects on males and females are favoured in one sex but disfavoured in the other [1, 4–8]. The intersexual genetic tug-of-war ensuing from such "sexual antagonism" [9, 10] can result in a fitness load as both sexes are displaced from their optimal phenotypes [1, 11] and has been proposed as a prominent source of balancing selection, driving the maintenance of genetic variation [10, 12–15]. This has led to the suggestion that sexual antagonism could explain patterns of elevated genetic variation within, and even between, species [1, 10, 16] ([17–19] for empirical examples).

Population genetic models have proved key to predicting the conditions under which sexually antagonistic balancing selection and elevated genetic polymorphism arise [12–14, 20–36]. These models typically consider one or a very small number of genetic loci and assume that the alleles segregating at these sites have fixed fitness effects (or selection coefficients, though see [9, 10] for models where selective effects are determined by the fitness landscape). These assumptions lead to tractable evolutionary dynamics from which the consequences of sexually antagonistic selection can be characterised. One salient point from this theory is that sexual antagonism can maintain genetic variation at a locus either when selection is strong, or when allelic dominance is sex-specific such that alleles are dominant when beneficial and recessive when deleterious ("sex-specific dominance reversal" [12, 14, 30]). Because such dominance relationships may result from fitness landscapes declining slowly away from phenotypic optima (i.e. showing diminishing returns to adaptation [37], as found on Gaussian fitness landscapes), multiple authors have suggested that favourable conditions for sexually antagonistic polymorphism may be common, especially in well-adapted populations [5, 10, 14, 15, 30, 38–43] (where landscapes typically show diminishing returns [44, 45]).

Here we assess whether intralocus conflict can maintain genetic polymorphism when sexually antagonistic selection acts on traits rather than individual loci with fixed fitness effects. We analyse genetically explicit models of a trait with divergent sex-specific optima. We investigate how sexually antagonistic selection influences the maintenance of genetic variation on different fitness landscapes and for different genetic architectures. In our models, the fitness effects of alleles are not fixed, but rather emerge from the genotype-phenotype map and the fitness landscape, under the assumption that alleles have the same phenotypic effects on males and females. Sexual antagonism therefore arises here because each sex favours a different optimal phenotype (as opposed to because alleles encode sex-specific phenotype effects, as in [46]).

2 Model

2.1 Life-cycle, traits, and fecundity

We consider a diploid population of large and constant size that is composed of equal numbers of adult males and females. At each generation, adult males and females produce large numbers of gametes that fuse randomly to produce zygotes. These zygotes become male and female juveniles with equal probability (so the sex ratio at birth is unbiased). Adults die and juveniles compete randomly within each sex to become the male and female adults of the next generation.

Each individual expresses a continuous trait, $z \in \mathbb{R}$, that influences their fitness. We assume that in both sexes there is an optimum trait value, which is $-\theta$ for males and θ for females (so that $\theta > 0$ controls the divergence in sex-specific optima). We consider a scenario where the trait influences the number of gametes produced (i.e. fecundity), but the trait effect on fitness could equivalently be through survival. The number, $w_{\mathrm{m}}(z)$, of sperm cells produced by a male with trait z, and the number, $w_{\mathrm{f}}(z)$, of egg cells produced by a female with trait z are given by

$$\begin{aligned} w_{\mathrm{m}}(z) &= K_{\mathrm{m}}\left(1 - s_{\mathrm{m}}\left[1 - \left(\frac{\theta - z}{2\theta}\right)^{b_{\mathrm{m}}}\right]\right) \\ w_{\mathrm{f}}(z) &= K_{\mathrm{f}}\left(1 - s_{\mathrm{f}}\left[1 - \left(\frac{\theta + z}{2\theta}\right)^{b_{\mathrm{f}}}\right]\right) \end{aligned} \tag{1}$$

where K_{m} and K_{f} are the maximum number of gametes produced by a male and a female (both assumed to be large). Equation (1) describes how fecundity diminishes with the distance between an individual's expressed phenotype, z, and its sex-specific optimum (Fig. 1). Specifically, $w_{\mathrm{m}}(z)$ decreases from K_{m} to $(1 - s_{\mathrm{m}})K_{\mathrm{m}}$ as z increases from $-\theta$, whereas $w_{\mathrm{f}}(z)$ decreases from K_{f} to $K_{\mathrm{f}}(1 - s_{\mathrm{f}})$ as z decreases from θ. The coefficients of selection $0 \leq s_{\mathrm{m}} \leq 1$ and $0 \leq s_{\mathrm{f}} \leq 1$ tune the steepness of this decline in each sex (see [12, 14] for a similar approach for a single locus). Finally, b_{m} and b_{f} control the shape of the sex-specific fecundity curves between θ and $-\theta$. When $b_{\mathrm{m}} = 1$ and $b_{\mathrm{f}} = 1$, fecundity changes linearly with z. When $b_{\mathrm{m}} > 1$ and $b_{\mathrm{f}} > 1$, the fecundity returns to adaptation in each sex accelerate towards the optimum (i.e. w_{m} and w_{f} are convex and increase in an accelerating manner as z approaches $-\theta$ and θ, respectively). Conversely, adaptation leads to diminishing returns towards the optimum in each sex when $b_{\mathrm{m}} < 1$ and $b_{\mathrm{f}} < 1$ (i.e. w_{m} and w_{f} are concave and increase in a decelerating manner as z approaches $-\theta$ and θ, respectively) similarly to Gaussian landscapes often used in quantitative genetic models (e.g. [9–11, 38, 47]), with the advantage that here the shape of the landscape $(b_{\mathrm{m}}, b_{\mathrm{f}})$ and the strength of selection $(s_{\mathrm{m}}, s_{\mathrm{f}})$ can be tuned independently. Throughout, we assume that z is bounded to $-\theta \leq z \leq \theta$ so that our analyses are focused to the region of trait space intermediate of the male and female optima, i.e. the "arena" for sexual conflict [48].

2.2 Trait genetic architecture and evolution

We analyse two complementary versions of the above model, which provide different and complementary insights into the evolution of antagonistic traits by making different assumptions about the genetic basis of z. First, to characterise the nature of selection at the phenotypic level (i.e. ignoring genetic constraints on allelic variation) that arises from the male- and female-specific fecundity curves, we follow Kimura's continuum-of-alleles [49] model. This encodes z by a single additive locus and follows its evolution through mutations that create new alleles whose value deviates from the original allele by a small amount (see Appendix A for details). When mutations are rare, phenotypic evolution occurs in two phases in this model [50–53]. Initially, the population evolves under directional selection whereby positively selected mutations rapidly sweep to fixation so that the population transits from being largely monomorphic for one trait value to being monomorphic for another. The population may thus eventually converge to an intermediate singular trait value $z^* \in [-\theta, \theta]$. Then, selection is either stabilising so that the population remains unimodally distributed around z^* [54], or diversifying, which leads to the emergence of highly differentiated allelic values at the evolving locus (i.e. negative frequency dependent disruptive selection leading to "evolutionary branching" [50, 52, 55, 56]).

Second, to investigate how selection at the phenotypic level affects polygenic variation, we assume that z is encoded by L additive loci that are equally distributed across a single pair of large chromosomes. The phenotype expressed by an individual of either sex is given by

$$z = \sum_{k=1}^{L} (x_{k,1} + x_{k,2}) \tag{2}$$

where $x_{k,1}$ and $x_{k,2}$ are the allelic values carried at the paternal and maternal copy at locus k, respectively. Genetic effects on phenotype are thus additive within and between loci, but depending on fecundity curves (Eq. 1), they may translate into epistatic and dominance effects on fitness. We assume that z is encoded by multiple loci ($L > 1$) and that each locus $k \in \{1, \ldots, L\}$ has two possible alleles, A_k and a_k. Allele A_k increases the size of the trait z and allele a_k decreases it. Specifically, the effect of the allelic copy $x_{k,l}$ inherited from parent $l \in \{1, 2\}$ at locus k is

$$x_{k,l} = \begin{cases} \delta_k, & \text{if allele } \mathrm{A}_k \text{ is present} \\ -\delta_k, & \text{if allele } \mathrm{a}_k \text{ is present} \end{cases} \tag{3}$$

where $\delta_k > 0$ is the absolute phenotypic contribution of a single allele at the locus. We initially assume that each locus contributes equally, with $\delta_k = \delta$ for all k, so that the maximum and minimum phenotypes are $\theta = 2\delta L$ and $\theta = -2\delta L$, respectively. Females express their optimal phenotype (θ) when homozygous for allele A_k at every locus k, while males express their optimal phenotype ($-\theta$) when homozygous for a_k at every locus (Fig. 1). With $L = 1$, this model reduces to classic single-locus population genetic models (e.g. [12, 14, 26], see Appendix B), and with many loci of small effects ($L \to \infty$ and $\delta \to 0$) to quantitative genetic models of sexual antagonism (e.g. [11] in the absence of environmental effects on phenotype and with cross-sex genetic correlation equal to one). Mutations from A_k to a_k and from a_k to A_k occur at a per-locus rate of μ and we assume recombination

is free between adjacent loci (i.e. occurs at a rate $r = 0.5$).

We analyse our models through a combination of mathematical and numerical approaches that are detailed in the Appendix. To simplify presentation, we focus in the main text on the case where fecundity curves have the same shape in both sexes ($b_m = b_f = b$). In Appendix C, we relax this assumption by allowing for sex-specific fecundity curves ($b_m \neq b_f$ in eq. 1). We also relax some of our genetic assumptions, allowing for loci to have variable effect sizes (i.e. variation in δ_k across k to model the presence of large and small effect loci) and for genetic linkage (i.e. $r < 0.5$). Finally, we investigate the evolutionary dynamics of our model under more general fitness functions (i.e. under arbitrary functions $w_m(z)$ and $w_f(z)$). Overall, we find that none of these departures from our baseline model have a significant influence on the results presented below (as detailed later in our Discussion).

3 Results

3.1 Sexual antagonism generates directional, stabilising, and diversifying selection

For the continuum-of-alleles model, we show in Appendix A that depending on the shape of the fecundity curves (eq. 1), evolutionary dynamics under sexual antagonism can proceed in three ways that each reflect a distinct mode of selection on the trait z (Fig. 2A for summary when $s_m = s_f$).

First, when fecundity curves are diminishing ($b < 1$, Fig. 2A, purple region), the population converges and remains distributed around an intermediate singular trait value $z^* \in [-\theta, \theta]$ (Fig. 2B, solid curve) owing to stabilising selection (Fig. 2C). This stable attractor is given by

$$z^* = \theta \cdot \frac{1 - (s_m/s_f)^{1/(1-b)}}{1 + (s_m/s_f)^{1/(1-b)}} + \mathcal{O}(\epsilon^2), \tag{4}$$

where $\epsilon > 0$ is a parameter of the order of s_m and s_f. As eq. (4) shows, asymmetry in the strength of sex-specific selection leads z^* to move closer to the optimum of the sex under stronger selection (i.e. z^* gets closer to $-\theta$ as s_m/s_f increases, closer to θ as s_m/s_f decreases, and $z^* = 0$ when $s_m/s_f = 1$, Fig. 2B solid curve). Selection is stabilising here because with diminishing curves ($b < 1$) the intermediate phenotype z^* confers higher average fitness across the sexes than more extreme phenotypes.

Second, when fecundity curves are accelerating ($b > 1$) and selection is either weak (Fig. 2A, yellow region) or stronger in one sex than the other ($s_m \neq s_f$, Supplementary Fig. 1 top row panels), the singular intermediate trait value z^* (eq. 4) is not an attractor of evolutionary dynamics but a repellor. In this case, selection is directional, pushing z away from z^* and towards being monomorphic for either the male optimum ($-\theta$) or the female optimum (θ), depending on the initial value of z in the population relative to z^* (Fig. 2D for an example). This is because accelerating curves cause intermediate phenotypes to have low fitness when averaged across

males and females. Selection against these phenotypes therefore favours adaptation in one sex at the expense of the other. Here, differences in the strengths of sex-specific selection (s_m and s_f) shift z^* further away from the optimum of the more strongly selected sex (eq. 4 with $b > 1$), thus increasing the basin of attraction of evolutionary dynamics towards the optimum of that sex (Fig. 2B, dashed curve). The population is thus more likely to evolve the optimal trait value of the sex under stronger selection (i.e. θ when $s_m < s_f$ and $-\theta$ when $s_m > s_f$).

Third, when curves are accelerating ($b > 1$) and selection is both strong and symmetrical across sexes (s_m and s_f are large and similar, green regions in Fig. 2A and Supplementary Fig. 1 top row panels), the population first converges towards z^* (eq. 4) but then becomes polymorphic owing to diversifying selection (Fig. 2E). Such diversifying selection is generated by the tension between, on one hand, selection across both sexes against intermediate phenotypes (owing to $b > 1$), and, on the other, strong selection within each sex against extreme phenotypes, i.e. against $-\theta$ in females and θ in males (owing to large s_m and s_f; see Appendix A for details). This leads to the emergence and stable maintenance of two differentiated alleles: a male-beneficial and a female-beneficial allele, which in turn drives a sharp increase in phenotypic and fitness variance within each sex (Fig. 2F-G).

3.2 Sexual antagonism diminishes polygenic variation unless selection is diversifying

To investigate the response to sexually antagonistic selection when z is underlain by multiple genes, we used individual-based simulations of the polygenic model (eq. 2 with eq. 3). We did so for a population of size $N = 10^4$ and across a wide range of parameter values that modulate genetic conflict (within $b \in [0.25, 3]$, $s_m \in [0, 1]$, $s_f \in [0, 1]$, $L \in [1, 50]$, and θ fixed for 1, Appendix B.3 for details). Simulations were initialised with equal frequencies of both alleles at each locus and run for 10^5 generations, which was always enough to reach mutation-selection-drift equilibrium. Genetic variation was quantified as average heterozygosity across all loci contributing to z at equilibrium, which we compared with the heterozygosity expected at a neutral locus (i.e. $H = 4N\mu/[1 + 8N\mu]$, e.g. eq. 2.24 in [57] with their $k = 2$). These analyses showed that sexual antagonism leads to three broad patterns of heterozygosity that correspond to whether selection on phenotype is directional, stabilising, or diversifying, as characterised by the continuum-of-alleles model (Fig. 2A).

First, when fecundity curves are such that selection is directional, average heterozygosity is much lower than expected at neutrality and often close to zero (Fig. 3A). This is because, by continuously pushing for the optimum of one sex, directional selection favours the fixation of either all A or all a alleles across loci in the population and then tends to quickly eliminate any deviating mutant allele.

Second, when fecundity curves produce stabilising selection for intermediate trait value z^* (eq. 4), average heterozygosity is greater than under directional selection but still below that of a neutral locus (Fig. 3A). Here, heterozygosity is pushed below neutral levels because stabilising selection favours genotypes that encode the equilibrium phenotype in homozygote state (an effect already well-known to occur under sex-concordant sta-

bilising selection [46, 58, 59]). Specifically, while z^* can be produced by multiple genotypes, including heterozygotes (e.g. Fig. 1 for $L = 2$), homozygote genotypes are favoured because they produce offspring that, on average, are more likely to express z^* and are thus themselves fitter. In other words, although homozygote and heterozygote genotypes expressing z^* can both expect the same number of offspring, homozygote genotypes are less likely to be broken down by random Mendelian segregation and so experience a weaker segregation load. Carriers of homozygote genotypes therefore have on average more grand-offspring than carriers of heterozygote genotypes. In a polygenic trait, this leads selection to drive the fixation of a combination of A and a alleles across loci (depending on z^*, e.g. equal numbers of loci fixed for each allele when $z^* = 0$), with transient variation at individual loci being maintained at mutation-selection-drift balance (Supplementary Fig. 2A).

Although stabilising selection reduces the average heterozygosity across loci relative to neutrality, in some instances we observe the stable maintenance of a genetic polymorphism at a maximum of one locus (out of the L that code for the trait, Fig. 3B). This occurs whenever no homozygote genotype codes for a phenotype that is close enough to z^* to fix ([59] for a description of this under sex-concordant selection). Selection then favours fixation of alleles at all loci except one remainder locus that stays polymorphic. Polymorphism is maintained in this case due to sex-specific dominance reversal: owing to the diminishing shape of the fecundity curves ($b < 1$), both alleles at the remainder locus have a larger effect in the sex they benefit than in the sex they harm (see Fig. 3C for a graphical representation and Appendix B.2.2 for analysis of $L = 2$ case). However, unless selection is particularly strong, genetic drift and recurrent mutation drive a turnover in the identity of the remainder locus, so that any one site shows only transient polymorphism (Supplementary Fig. 2B).

Finally, average heterozygosity is significantly greater than under neutrality when fecundity curves are such that selection is diversifying (Fig. 3A). This is because diversifying selection favours the evolution and maintenance of male- and female-adapted genotypes composed of different alleles at many (if not all) loci, thus maintaining genetic polymorphism across sites. Moreover, because genetic variation is shuffled by Mendelian segregation and recombination at each generation, diversifying selection leads to a wide distribution of phenotypes among individuals that is increasingly smooth and continuous as the number (L) of underlying trait loci increases (Fig. 3D). The highest levels of heterozygosity and phenotypic variation are observed under conditions where diversifying selection is the most intense, i.e. where (i) fecundity curves are strongly accelerating ($b \gg 1$), as this entails that intermediate genotypes show especially low fecundity; combined with (ii) exceptionally strong sexual antagonism ($s_\mathrm{m} \sim 1$ and $s_\mathrm{f} \sim 1$) to oppose the fixation of the male or female-adapted genotypes (Fig. 3A). In addition, selection is most effective in driving elevated heterozygosity when the number L of loci that contribute to the trait is small relative to population size. This is because otherwise evolution at each individual locus becomes dominated by genetic drift (Supplementary Fig. 3).

3.3 Sexual antagonism produces weak genomic signatures

To investigate whether sexually antagonistic selection at quantitative trait loci produces signatures that may be found in genetic sequence data, we analysed the simulated data from our polygenic model using two population genomic approaches that are commonly leveraged to identify sexually antagonistic loci (Appendix D for full procedures and calculations). First, we tested whether sexually antagonistic selection drives allelic differentiation between the sexes. This is typically quantified as between-sex F_{ST} [16, 60–64], which in the context of sexually antagonistic fecundity selection is measured amongst the successful parents in a given generation [64]. Second, we tested whether sexually antagonistic selection leads to detectable associations between allelic state and sex-specific fitness, as in GWAS for sex-specific fitness and sexual antagonism [18, 63, 65]. To quantify sex-differences in fitness associations, we computed $|\beta_{\mathrm{m},k} - \beta_{\mathrm{f},k}|$ for every locus k where $\beta_{\mathrm{m},k}$ and $\beta_{\mathrm{f},k}$ are the linear regression of reproductive success (i.e. number of recruited offspring) in males and females, respectively, against within-individual frequency of allele A at locus k.

We focused on two cases where we expect to see sufficient genetic variation at mutation-selection-drift balance to perform statistical calculations: (i) where fecundity curves lead to diversifying selection; and (ii) where they lead to stabilising selection around $z^* = 0$. As controls, we computed allelic differentiation and sex-specific fitness associations from our simulations with individual sex identity randomly assigned during statistical calculations. This allows us to compare the effects of sexual antagonism with cases where the total genetic variation is identical, but not distributed differently between males and females (in expectation). In line with recent work on detecting sexually antagonistic polymorphisms (reviewed in [63, 64]), our aim in this section is to investigate to what extent sexually antagonistic selection produces distinct distributions of test values (F_{ST} and $|\beta_{\mathrm{m},k} - \beta_{\mathrm{f},k}|$) than under neutrality.

We find that between-sex allelic differentiation is generally weak for quantitative trait loci under sexually antagonistic selection and that the distribution of F_{ST} across loci is in fact largely similar to that under neutrality or where sex is randomly assigned (Fig. 4A). This is expected, as generating appreciable between-sex F_{ST} values typically requires strong sex-specific selection acting on a given locus [62, 66] and sexually antagonistic selection acting on a polygenic trait translates into weak effects on each individual locus. One exception is where sexual antagonism causes strong diversifying selection (Fig. 4A, green boxplots). This leads to elevated allelic differentiation among the sexes, albeit still significantly below that suggested by single locus models (e.g. at a single locus, $s_{\mathrm{m}} = s_{\mathrm{f}} = 0.6$ generates F_{ST} of the order of 10^{-2}, see Figure 5 in [62], when in our model with $L = 10$, this generates F_{ST} of the order 10^{-4}, Fig. 4A). This indicates that measures of genetic differentiation such as sex-specific F_{ST} will produce a signal for sexually antagonistic quantitative trait loci only under the relatively extreme biological scenarios that lead to diversifying selection and that detecting this likely requires the availability of particularly large datasets or methods that combine F_{ST} patterns across the genome (e.g. by relating to the degree of biased gene expression [61]).

When feasible, performing genetic associations with fitness may offer a more productive approach. Indeed, we

observe that compared to controls, sexual antagonism drives an increase in $|\beta_{\mathrm{m},k} - \beta_{\mathrm{f},k}|$ when selection is either stabilising or diversifying, so long as selection is sufficiently strong (i.e. s_{m} and s_{f} not too small, Fig. 4B). Sex-specific fitness associations are possible when selection is stabilising for z^* because fecundity curves in each sex can be steep close to z^* (e.g. see Fig. 1 Top where $z^* = 0$). As a consequence, segregating genetic variation can covary noticeably with male and female fitness in opposite ways. However, detecting sexually antagonistic loci when stabilising selection is strong may prove challenging because most loci either fix or show low minor allele frequency in this case (Fig. 4C), leaving them unamenable to statistical calculations unless large volumes of data are available.

4 Discussion

Our analyses indicate that there are two routes for sexual antagonism to maintain balanced polymorphisms. The first is where sexual antagonism causes stabilising selection for an intermediate phenotype that is not attainable as a homozygote genotype. Selection maintains a balanced polymorphism at a maximum of one locus in this case, where a combination of diminishing sex-specific fitness curves ($b < 1$, Fig. 1 Top) and effect sizes across loci generate sex-specific dominance reversal at the polymorphic locus [12, 14, 15]. The second route to balancing selection is via diversifying selection. Here, balancing selection can act at many individual loci because the male- and female-adapted genotypes that are favoured by diversifying selection are composed of different alleles across many or all loci contributing to the trait. For polymorphism to arise in this way, fitness curves need to be accelerating in both sexes ($b > 1$, Fig. 1 Bottom), and sex-specific selection needs to be both very strong and of similar intensity in males and females.

A key insight from our model is therefore that the conditions under which selection traits can maintain sexually antagonistic genetic variation across loci are restrictive. For example, to observe an average heterozygosity greater than 0.3 over ten quantitative trait loci ($L = 10$) requires roughly that $s_{\mathrm{m}} \approx s_{\mathrm{f}} > 0.5$ (Fig. 3C). In other words, individuals expressing their least-favoured phenotype must suffer at least a 50% drop in fecundity. Only then is selection strong enough to generate the negative frequency-dependence required for the invasion at multiple loci of mutant alleles that are beneficial to one sex into populations where alleles beneficial to the other sex are common. In addition, when selection is strong enough to maintain sexually antagonistic polymorphism, we do not expect such polymorphism to last over substantial evolutionary periods. To see this, consider that owing to random Mendelian segregation, phenotypic variation in a polymorphic population remains distributed around an intermediate value (Fig. 3D) that confers low fitness in both sexes. This imposes a large sex load, which generates strong selection to resolve sexual conflict [1, 11] (through e.g. the evolution of sex-specific gene expression [67]). Therefore, where sexual antagonism does drive balanced polymorphism across loci, such selection is unlikely to persist over evolutionary time unless there are important constraints on the evolution of phenotypic plasticity that preclude sexual dimorphism [68].

Where selection is not strong enough to generate diversifying selection, our model shows that sexual antag-

onism erodes polymorphism across loci through stabilising or directional selection on the trait. This finding is consistent with existing theory of sex-concordant concordant selection, i.e. in the absence of sexual conflict over trait values (e.g. monoecious populations or dioecious populations where the fitness landscape is the same in males and females). Such models predict that stabilising selection erodes genetic variation (reviewed in [46, 58, 59], chap. 28 in [57], see also [69] for fluctuating selection) and that, in the absence of tight linkage between loci, selection typically maintains a maximum of one polymorphic site (e.g. [59, 70–73]), including where alleles have sex-specific phenotypic effects [46]. This is because heterozygote genotypes are more easily broken down by Mendelian segregation, resulting in a wider distribution of phenotypes among offspring, some of which deviate from the optimum under stabilising selection and so are less fit. Our results also echo studies exploring the conditions for local adaptation to different environments to maintain polymorphism in the face of dispersal (e.g. [74–78]). In these models, dispersal must fall below a critical threshold relative to selection, otherwise selection is stabilising for a single optimum and so disfavours allelic variation. Our model is in fact equivalent to a model of local adaptation with two patches where selection is soft and between which dispersal is random (equal to $1/2$). From this perspective, it is then not so surprising that only very strong selection can maintain polymorphism here.

Our results therefore reinforce the general notion that, whatever its source, stabilising selection erodes variation by favouring intermediate homozygote genotypes over intermediate heterozygote genotypes. Moreover, even when allelic variation is such that stabilising selection leads to the maintenance of variation at a single locus, we find that this is in fact unlikely to drive long-term polymorphism at any given genetic site. This is first because mutation and drift drive regular turnover in the identity of the remainder locus unless selection is very strong (Supplementary Fig. 2), and second because such polymorphism is not robust to the appearance of new alleles that encode the optimal phenotype when homozygous. In this way, just as when selection diversifying, sexually antagonistic polymorphism can only be maintained in the long run because of genetic constraints, this time on the possible allelic variants that may arise at an antagonistic locus.

While our model takes an idealised view of the genetic basis of phenotypic variation, our key conclusions are largely independent of several important simplifying assumptions. First, in line with classic quantitative genetics [57, 79], our main polygenic model considers that the trait z is encoded by freely recombining loci with equal phenotypic effects. In Appendices C.2-C.3 we show our results are robust to deviations from these baseline assumptions. Specifically, variation in effect sizes (δ_k) simply alters the phenotypes expressed by different homozygote genotypes. Under stabilising selection, this may affect which genotypes are close to the optimum z^* and therefore whether any loci or which locus eventually remains polymorphic. But it is still the case that ultimately a maximum of one locus experiences balancing selection. Similarly, decreasing the recombination rate between loci ($r < 0.5$) has little effect on the conditions for polymorphism, with the exception of extremely tight linkage relative to selection. In this case, polymorphism across multiple loci is more easily maintained under stabilising selection, as polygenic haplotypes behave increasingly like a single locus and the behaviour of the system approaches the classic single-locus model. Second, we also assumed that the trait z has a purely

genetic basis. In reality, however, quantitative traits often show some environmental dependence [80, 81], and this is especially true for sexual phenotypes, which commonly show condition-dependence [82–85]. By producing non-heritable variation, environmental effects should dampen the impact of sexually antagonistic selection on genetic variation, making it less likely for such selection to be able to maintain elevated polymorphism. By excluding such effects, our model therefore represents the best-case scenario for the maintenance of sexually antagonistic polymorphism.

One important assumption in our model was that loci have additive effects on the phenotype. Epistatic genetic effects on fitness therefore arise due to the mapping of phenotype to fitness, but these are an emergent property. Introducing arbitrary epistatic variation directly at the phenotypic level (i.e. non-additive phenotypic effects caused by specific interactions between genes [86, 87]) will alter the fitness of different genotypes and thus may impact the conditions for maintaining polymorphism [88–90]. Indeed, such epistatic effects explain some of the discrepancies between our results and those from previous two-locus models of sexual antagonism, where genotypic fitness follows a sex-specific multiplicative model [24, 25] (with the addition of multiplicative epistasis in [30]). The increased genetic complexity of these models generates more permissive conditions for polymorphism because double heterozygotes can experience an intrinsic fitness advantage under certain parameter values, which does not arise in our additive quantitative trait approach. While it is unclear how easily such multiplicative fitness effects can extend over many loci for the same trait, these results suggest that there may exist scenarios where polymorphism is more readily favoured than in our model.

Nevertheless, our analysis in Appendix C.4 of sexually antagonistic variation under arbitrary fitness functions indicates that particular scenarios capable of maintaining polymorphism do not arise easily. Specifically, we show that when variation in the fecundity of each sex is weak, there exist no combination of male and female fecundity functions, $w_{\mathrm{m}}(z)$ and $w_{\mathrm{f}}(z)$, such that polymorphism gradually emerges from small mutational changes (i.e. selection is never diversifying, whatever the functions $w_{\mathrm{m}}(z)$ and $w_{\mathrm{f}}(z)$; C.4.1). Furthermore, we show that even though there exists some fecundity functions such that a pre-existing polymorphism of two strongly diverged alleles can be maintained at one locus (C.4.2), such polymorphism immediately breaks down when traits are encoded by multiple loci (Appendix C.4.3).

By making general predictions about the maintenance of sexually antagonistic genetic variation, our analysis provides several insights for empirical work on sexually antagonistic polymorphism. First, our results indicate that traits under sexually antagonistic selection will typically exhibit relatively little additive genetic variation. This is because antagonistic selection, unless it is very strong, tends to be stabilising and so leads to an erosion of genetic variation even compared to the level expected under mutation-drift balance. Where sexually antagonistic traits are found to show high levels of standing variation, we expect such traits to be under strong selection with accelerating fitness curves in both sexes, two necessary conditions for generating diversifying selection. Empirically, this could be tested directly by fitting quadratic regressions of reproductive success on trait values in each sex [54]. We note, however, that non-linear selection gradients on sexually antagonistic traits are rarely significant (e.g. [91–93]), likely due to the requirement of large datasets to detect second-order

fitness effects. In principle, the effect of sexual antagonism on levels of genetic variation could also be assessed experimentally, by measuring the impact of manipulating the strength and nature of antagonistic selection on levels of additive genetic variation for fitness. Studies using family-based selection for sexual dimorphism (e.g. [43, 94]) provide templates for such an approach. One such study [43] found that standing genetic variation did decrease under antagonistic selection, albeit less so than under other modes of selection.

At the genetic level, our results suggest that antagonistic selection on continuous traits leaves few signatures in patterns of polymorphism within populations—except in the presence of diversifying selection (Fig. 4). Therefore, in most cases, genetic signatures of sexual antagonism will be very subtle and correspond mostly to allelic variation that is maintained due to mutation and drift. Whether and to what extent these signals are detectable will depend on circumstances. Most importantly, detectability will depend on a number of experimental parameters that have predictable effects on statistical power and that we have not explored here, such as sample size and the degree of environmental noise in the trait. Beyond these, our results indicate that the approach used to detect genetic signatures will have a major impact on power. We find that methods based on between-sex genetic differentiation (e.g. sex-specific F_{ST} [16, 60–64]) have very low power to detect individual trait loci [62], as such a signal is based on frequency change over a single generation and selection on individual loci underlying a polygenic trait is weak (although this may be less problematic for approaches looking at genome-wide signs of sex-specific selection and so gain power across loci [61]). Meanwhile, approaches based on gene-fitness associations (e.g. GWAS for sex-specific fitness [18, 63, 65]) are more powerful—relatively speaking. The small per-locus effects of sexual antagonism also compromise their usefulness where selection is weak. Finally, both sex-specific F_{ST} and GWAS-type approaches are constrained by the fact that, unless it drives diversifying selection, strong sexual antagonism reduces genetic variation and so leaves few loci at which any detectable signal of sexual conflict would be present. Indeed, these signals may easily be drowned in genomic background noise, unless a candidate set of loci is known. And even where a locus is detected, this would necessarily provide a poor picture of the loci that are subject to antagonistic selection—which includes those showing no excess, or a complete absence of, variation.

A corollary of the widespread loss of polymorphism under antagonistic selection is that, where multiple sexually antagonistic loci showing elevated genetic variation are identified, these most likely underlie different traits. Given this prediction, it is of little surprise that antagonistic loci detectable by GWAS approaches show no functional enrichment [18]. Additionally, the predicted turnover in the identity of trait loci harbouring polymorphism at any given time under stabilising selection fits with the observation that polygenic variation underlying traits under antagonistic selection shows little signal of long-term balancing selection [64, 95]. Our results therefore suggest that the rare loci where a strong signal of antagonism and balancing selection is detectable are expected to be those showing large phenotypic (and hence fitness) effects. It is these loci that are most likely to generate the genetic constraints that are necessary to maintain long-term polymorphism under stabilising selection across the sexes. Indeed this is true for allelic variants at the *VGLL3* gene in Atlantic salmon that generate a sexually antagonistic polymorphism in maturation time and account for 39% of trait variation [96].

Similarly, large and experimentally replicable effects were demonstrated in a locus that underlies a sexually antagonistic polymorphism in cuticular hydrocarbon profiles in the tropical fly *Drosophila serrata* and that shows signatures of balancing selection [97].

5 Conclusion

Previous theory on sexual antagonism has relied overwhelmingly on models of Mendelian traits that are determined by a limited number of alleles with fixed effects [12–14, 20–36]. This reliance may have led to the common expectation that sexually antagonistic genetic polymorphisms are a regular feature of sexual species [10, 13–15, 30, 40, 41, 43] and that such polymorphisms should be detectable from genomic data (provided the availability of large sample sizes and sufficiently strong sexual conflict [16, 63, 98]). But our work has shown that this expectation rarely extends to continuous traits. By considering some of the complexity of polygenicity, specifically the presence of multiple interacting alleles whose fitness effects are the product of genotype-phenotype maps and fitness landscapes [57, 79], our model demonstrates that key previous conditions for balancing selection are direct consequences of restricting the number and the nature of alleles that can affect a trait. These conditions do not generalise to cases where a wider variety of alleles can arise either within or across loci. In fact, our analyses indicate that sexual antagonism is not a straightforward driver of the long-term maintenance of polymorphism at loci underlying complex traits and thus rarely produces distinctive patterns of variation. We therefore suggest that most sexually antagonistic polymorphisms associated with quantitative trait loci are transient, and should be observed no more frequently than at neutral sites.

Acknowledgements. We thank Seth Watt for extensive discussions about evolution with sex-differences in selection and for exploring and sharing early simulations with different fitness functions not included here. We also thank Tim Connallon, Filip Ruzicka and Carl Mackintosh for useful discussion.

Funding. We are grateful to the Swiss National Science Foundation (PCEFP3181243 to CM), the Biotechnology and Biological Sciences Research Council (BB/W007703/1 to MR), the Natural Sciences and Engineering Research Council of Canada (NSERC RGPIN- 2022-03726 to SPO), and the Natural Environment Research Council (NERC grant to VS) for funding.

References

[1] Bonduriansky R, Chenoweth SF. 2009 Intralocus sexual conflict. *Trends in ecology & evolution* **24**, 280–288.

[2] Cox RM, Calsbeek R. 2009 Sexually antagonistic selection, sexual dimorphism, and the resolution of intralocus sexual conflict. *The American Naturalist* **173**, 176–187.

[3] Poissant J, Wilson AJ, Coltman DW. 2010 Sex-specific genetic variance and the evolution of sexual dimorphism: a systematic review of cross-sex genetic correlations. *Evolution* **64**, 97–107.

[4] Parker G et al.. 1979 Sexual selection and sexual conflict. *Sexual selection and reproductive competition in insects* **123**, 166.

[5] Rice W, Chippindale A. 2001 Intersexual ontogenetic conflict. *Journal of Evolutionary Biology* **14**, 685–693.

[6] Chapman T, Arnqvist G, Bangham J, Rowe L. 2003 Sexual conflict. *Trends in Ecology & Evolution* **18**, 41–47.

[7] Arnqvist G, Rowe L. 2005 *Sexual Conflict* vol. 31. Princeton University Press.

[8] Van Doorn GS. 2009 Intralocus sexual conflict. *Annals of the New York Academy of Sciences* **1168**, 52–71.

[9] Connallon T, Clark AG. 2014a Evolutionary inevitability of sexual antagonism. *Proceedings of the Royal Society B: Biological Sciences* **281**, 20132123.

[10] Connallon T, Clark AG. 2014b Balancing selection in species with separate sexes: insights from Fisher's geometric model. *Genetics* **197**, 991–1006.

[11] Lande R. 1980 Sexual dimorphism, sexual selection, and adaptation in polygenic characters. *Evolution* **34**, 292–305.

[12] Kidwell J, Clegg M, Stewart F, Prout T. 1977 Regions of stable equilibria for models of differential selection in the two sexes under random mating. *Genetics* **85**, 171–183.

[13] Rice WR. 1984 Sex chromosomes and the evolution of sexual dimorphism. *Evolution* **38**, 735–742.

[14] Fry JD. 2010 The genomic location of sexually antagonistic variation: some cautionary comments. *Evolution: International Journal of Organic Evolution* **64**, 1510–1516.

[15] Connallon T, Chenoweth SF. 2019 Dominance reversals and the maintenance of genetic variation for fitness. *PLoS biology* **17**, e3000118.

[16] Mank JE. 2017 Population genetics of sexual conflict in the genomic era. *Nature Reviews Genetics* **18**, 721–730.

[17] Foerster K, Coulson T, Sheldon BC, Pemberton JM, Clutton-Brock TH, Kruuk LE. 2007 Sexually antagonistic genetic variation for fitness in red deer. *Nature* **447**, 1107.

[18] Ruzicka F, Hill MS, Pennell TM, Flis I, Ingleby FC, Mott R, Fowler K, Morrow EH, Reuter M. 2019 Genome-wide sexually antagonistic variants reveal long-standing constraints on sexual dimorphism in fruit flies. *PLoS biology* **17**, e3000244.

[19] Eyer PA, Blumenfeld AJ, Vargo EL. 2019 Sexually antagonistic selection promotes genetic divergence between males and females in an ant. *Proceedings of the National Academy of Sciences* **116**, 24157–24163.

[20] Owen A. 1953 A genetical system admitting of two distinct stable equilibria under natural selection. *Heredity* **7**, 97.

[21] Albert AY, Otto SP. 2005 Sexual selection can resolve sex-linked sexual antagonism. *Science* **310**, 119–121.

[22] Gavrilets S, Rice WR. 2006 Genetic models of homosexuality: generating testable predictions. *Proceedings of the Royal Society B: Biological Sciences* **273**, 3031–3038.

[23] Patten MM, Haig D. 2009 Maintenance or loss of genetic variation under sexual and parental antagonism at a sex-linked locus. *Evolution* **63**, 2888–2895.

[24] Patten MM, Haig D, Ubeda F. 2010 Fitness variation due to sexual antagonism and linkage disequilibrium. *Evolution* **64**, 3638–3642.

[25] Ubeda F, Haig D, Patten MM. 2011 Stable linkage disequilibrium owing to sexual antagonism. *Proceedings of the Royal Society B: Biological Sciences* **278**, 855–862.

[26] Connallon T, Clark AG. 2012 A general population genetic framework for antagonistic selection that accounts for demography and recurrent mutation. *Genetics* **190**, 1477–1489.

[27] Mullon C, Pomiankowski A, Reuter M. 2012 The effects of selection and genetic drift on the genomic distribution of sexually antagonistic alleles. *Evolution: International Journal of Organic Evolution* **66**, 3743–3753.

[28] Jaquiéry J, Rispe C, Roze D, Legeai F, Le Trionnaire G, Stoeckel S, Mieuzet L, Da Silva C, Poulain J, Prunier-Leterme N, Ségurens B, Tagu D, Simon JC. 2013 Masculinization of the X Chromosome in the Pea Aphid. *PLoS Genetics* **9**, e1003690–15.

[29] Jordan CY, Connallon T. 2014 Sexually antagonistic polymorphism in simultaneous hermaphrodites. *Evolution* **68**, 3555–3569.

[30] Arnqvist G, Vellnow N, Rowe L. 2014 The effect of epistasis on sexually antagonistic genetic variation. *Proceedings of the Royal Society B: Biological Sciences* **281**, 20140489.

[31] Spencer HG, Priest NK. 2016 The evolution of sex-specific dominance in response to sexually antagonistic selection. *The American Naturalist* **187**, 658–666.

[32] Hill MS, Reuter M, Stewart AJ. 2019 Sexual antagonism drives the displacement of polymorphism across gene regulatory cascades. *Proceedings of the Royal Society B* **286**, 20190660.

[33] Otto SP. 2019 Evolutionary potential for genomic islands of sexual divergence on recombining sex chromosomes. *New Phytologist* **224**, 1241–1251.

[34] Ruzicka F, Connallon T. 2020 Is the X chromosome a hot spot for sexually antagonistic polymorphisms? Biases in current empirical tests of classical theory. *Proceedings of the Royal Society B* **287**, 20201869.

[35] Hitchcock TJ, Gardner A. 2020 A gene's-eye view of sexual antagonism. *Proceedings of the Royal Society B* **287**, 20201633.

[36] Flintham EO, Savolainen V, Mullon C. 2021 Dispersal alters the nature and scope of sexually antagonistic variation. *The American Naturalist* **197**, 543–559.

[37] Manna F, Martin G, Lenormand T. 2011 Fitness landscapes: an alternative theory for the dominance of mutation. *Genetics* **189**, 923–937.

[38] Connallon T, Clark AG. 2010 Sex linkage, sex-specific selection, and the role of recombination in the evolution of sexually dimorphic gene expression. *Evolution: International Journal of Organic Evolution* **64**, 3417–3442.

[39] Arnqvist G. 2011 Assortative mating by fitness and sexually antagonistic genetic variation. *Evolution* **65**, 2111–2116.

[40] Grieshop K, Arnqvist G. 2018 Sex-specific dominance reversal of genetic variation for fitness. *PLoS Biology* **16**, e2006810.

[41] Grieshop K, Ho EK, Kasimatis KR. 2021 Dominance reversals, antagonistic pleiotropy, and the maintenance of genetic variation. *arXiv preprint arXiv:2109.01571*.

[42] Reid JM. 2022 Intrinsic emergence and modulation of sex-specific dominance reversals in threshold traits. *Evolution* **76**, 1924–1941.

[43] Kaufmann P, Howie JM, Immonen E. 2023 Sexually antagonistic selection maintains genetic variance when sexual dimorphism evolves. *Proceedings of the Royal Society B* **290**, 20222484.

[44] Martin G, Lenormand T. 2006 A general multivariate extension of Fisher's geometrical model and the distribution of mutation fitness effects across species. *Evolution* **60**, 893–907.

[45] Martin G, Elena SF, Lenormand T. 2007 Distributions of epistasis in microbes fit predictions from a fitness landscape model. *Nature genetics* **39**, 555–560.

[46] Turelli M, Barton N. 2004 Polygenic variation maintained by balancing selection: pleiotropy, sex-dependent allelic effects and G× E interactions. *Genetics* **166**, 1053–1079.

[47] Fisher RA. 1958 *The genetical theory of natural selection*. Oxford University Press.

[48] Parker GA. 2006 Sexual conflict over mating and fertilization: an overview. *Philosophical Transactions of the Royal Society B: Biological Sciences* **361**, 235–259.

[49] Kimura M. 1965 A stochastic model concerning the maintenance of genetic variability in quantitative characters.. *Proceedings of the National Academy of Sciences* **54**, 731–736.

[50] Metz J, Geritz S, Meszena G, Jacobs F, Van Heerwaarden J. 1996 Adaptive dynamics: a geometrical study of the consequences of nearly faithful reproduction. In *Stochastic and spatial structures of dynamical systems* pp. 183–231. North-Holland.

[51] Rousset F. 2004 *Genetic Structure and Selection in Subdivided Populations*. Princeton, NJ: Princeton University Press.

[52] Dercole F, Rinaldi S. 2008 *Analysis of evolutionary processes*. Princeton University Press.

[53] Avila P, Mullon C. 2023 Evolutionary game theory and the adaptive dynamics approach: adaptation where individuals interact. *Philosophical Transactions of the Royal Society B* **378**, 20210502.

[54] Lande R, Arnold SJ. 1983 The measurement of selection on correlated characters. *Evolution* pp. 1210–1226.

[55] Geritz SA, Kisdi E, Metz JA et al.. 1998 Evolutionarily singular strategies and the adaptive growth and branching of the evolutionary tree. *Evolutionary ecology* **12**, 35–57.

[56] Rueffler C, Van Dooren TJ, Leimar O, Abrams PA. 2006 Disruptive selection and then what?. *Trends in Ecology & Evolution* **21**, 238–245.

[57] Walsh B, Lynch M. 2018 *Evolution and selection of quantitative traits*. Oxford University Press.

[58] Bulmer M. 1971 The effect of selection on genetic variability. *The American Naturalist* **105**, 201–211.

[59] Bürger R, Gimelfarb A. 1999 Genetic variation maintained in multilocus models of additive quantitative traits under stabilizing selection. *Genetics* **152**, 807–820.

[60] Lucotte EA, Laurent R, Heyer E, Segurel L, Toupance B. 2016 Detection of allelic frequency differences between the sexes in humans: a signature of sexually antagonistic selection. *Genome Biology and Evolution* **8**, 1489–1500.

[61] Cheng C, Kirkpatrick M. 2016 Sex-specific selection and sex-biased gene expression in humans and flies. *PLoS Genetics* **12**.

[62] Kasimatis KR, Ralph PL, Phillips PC. 2019 Limits to genomic divergence under sexually antagonistic selection. *G3: Genes, Genomes, Genetics* **9**, 3813–3824.

[63] Ruzicka F, Dutoit L, Czuppon P, Jordan CY, Li XY, Olito C, Runemark A, Svensson EI, Yazdi HP, Connallon T. 2020 The search for sexually antagonistic genes: Practical insights from studies of local adaptation and statistical genomics. *Evolution letters* **4**, 398–415.

[64] Ruzicka F, Holman L, Connallon T. 2022 Polygenic signals of sex differences in selection in humans from the UK Biobank. *PLoS Biology* **20**, e3001768.

[65] Berger D, Grieshop K, Lind MI, Goenaga J, Maklakov AA, Arnqvist G. 2014 Intralocus sexual conflict and environmental stress. *Evolution* **68**, 2184–2196.

[66] Kasimatis KR, Nelson TC, Phillips PC. 2017 Genomic signatures of sexual conflict. *Journal of Heredity* **108**, 780–790.

[67] Mank JE. 2017 The transcriptional architecture of phenotypic dimorphism. *Nature Ecology & Evolution* **1**, 1–7.

[68] Muralidhar P, Coop G. 2023 Polygenic outcomes of sexually antagonistic selection. *bioRxiv* pp. 2023–03.

[69] Bürger R, Gimelfarb A. 2002 Fluctuating environments and the role of mutation in maintaining quantitative genetic variation. *Genetics Research* **80**, 31–46.

[70] Wright S. 1935 Evolution in populations in approximate equilibrium. *Journal of Genetics* **30**, 257–266.

[71] Robertson A. 1956 The effect of selection against extreme deviants based on deviation or on homozygosis: With Two Text-figures. *Journal of Genetics* **54**, 236–248.

[72] Barton NH. 1986 The maintenance of polygenic variation through a balance between mutation and stabilizing selection. *Genetics Research* **47**, 209–216.

[73] Gavrilets S, Hastings A. 1994 Dynamics of genetic variability in two-locus models of stabilizing selection.. *Genetics* **138**, 519–532.

[74] Meszéna G, Czibula I, Geritz SAH. 1997 Adaptive dynamics in a 2-patch environment: A toy model for allopatric and parapatric specation. *Journal of Biological Systems* **5**, 265–284.

[75] Lythgoe KA. 1997 Consequences of gene flow in spatially structured populations. *Genetics Research* **69**, 49–60.

[76] Spichtig M, Kawecki TJ. 2004 The maintenance (or not) of polygenic variation by soft selection in heterogeneous environments. *The American Naturalist* **164**, 70–84.

[77] Svardal H, Rueffler C, Hermisson J. 2015 A general condition for adaptive genetic polymorphism in temporally and spatially heterogeneous environments. *Theoretical Population Biology* **99**, 76–97.

[78] Schmid M, Rueffler C, Lehmann L, Mullon C. 2023 Resource variation within and between patches: Where exploitation competition, local adaptation and kin selection meet. .

[79] Charlesworth B, Charlesworth D. 2010 *Elements of Evolutionary Genetics*. Roberts and Company Publishers.

[80] Lynch M, Walsh B et al.. 1998 *Genetics and analysis of quantitative traits* vol. 1. Sinauer Sunderland, MA.

[81] Mackay TF, Stone EA, Ayroles JF. 2009 The genetics of quantitative traits: challenges and prospects. *Nature Reviews Genetics* **10**, 565–577.

[82] Rowe L, Houle D. 1996 The lek paradox and the capture of genetic variance by condition dependent traits. *Proceedings of the Royal Society of London. Series B: Biological Sciences* **263**, 1415–1421.

[83] Jennions MD, Moller AP, Petrie M. 2001 Sexually selected traits and adult survival: a meta-analysis. *The Quarterly Review of Biology* **76**, 3–36.

[84] Cornwallis CK, Uller T. 2010 Towards an evolutionary ecology of sexual traits. *Trends in Ecology & Evolution* **25**, 145–152.

[85] Dougherty LR. 2021 Meta-analysis reveals that animal sexual signalling behaviour is honest and resource based. *Nature Ecology & Evolution* **5**, 688–699.

[86] Phillips PC. 2008 Epistasis—the essential role of gene interactions in the structure and evolution of genetic systems. *Nature Reviews Genetics* **9**, 855–867.

[87] Huang W, Richards S, Carbone MA, Zhu D, Anholt RR, Ayroles JF, Duncan L, Jordan KW, Lawrence F, Magwire MM et al.. 2012 Epistasis dominates the genetic architecture of Drosophila quantitative traits. *Proceedings of the National Academy of Sciences* **109**, 15553–15559.

[88] Gimelfarb A. 1989 Genotypic variation for a quantitative character maintained under stabilizing selection without mutations: epistasis.. *Genetics* **123**, 217–227.

[89] Hermisson J, Hansen TF, Wagner GP. 2003 Epistasis in polygenic traits and the evolution of genetic architecture under stabilizing selection. *The American Naturalist* **161**, 708–734.

[90] Turelli M, Barton N. 2006 Will population bottlenecks and multilocus epistasis increase additive genetic variance?. *Evolution* **60**, 1763–1776.

[91] Lewis Z, Wedell N, Hunt J. 2011 Evidence for strong intralocus sexual conflict in the Indian meal moth, Plodia interpunctella. *Evolution* **65**, 2085–2097.

[92] Stearns SC, Govindaraju DR, Ewbank D, Byars SG. 2012 Constraints on the coevolution of contemporary human males and females. *Proceedings of the Royal Society B: Biological Sciences* **279**, 4836–4844.

[93] Tarka M, Åkesson M, Hasselquist D, Hansson B. 2014 Intralocus sexual conflict over wing length in a wild migratory bird. *The American Naturalist* **183**, 62–73.

[94] Kaufmann P, Wolak ME, Husby A, Immonen E. 2021 Rapid evolution of sexual size dimorphism facilitated by Y-linked genetic variance. *Nature Ecology & Evolution* **5**, 1394–1402.

[95] Sylvestre F, Mérot C, Normandeau E, Bernatchez L. 2023 Searching for intralocus sexual conflicts in the three-spined stickleback (Gasterosteus aculeatus) genome. *Evolution* **77**, 1667–1681.

[96] Barson NJ, Aykanat T, Hindar K, Baranski M, Bolstad GH, Fiske P, Jacq C, Jensen AJ, Johnston SE, Karlsson S et al.. 2015 Sex-dependent dominance at a single locus maintains variation in age at maturity in salmon. *Nature* **528**, 405.

[97] Rusuwa BB, Chung H, Allen SL, Frentiu FD, Chenoweth SF. 2022 Natural variation at a single gene generates sexual antagonism across fitness components in Drosophila. *Current Biology* **32**, 3161–3169.

[98] Rowe L, Chenoweth SF, Agrawal AF. 2018 The genomics of sexual conflict. *The American Naturalist* **192**, 274–286.

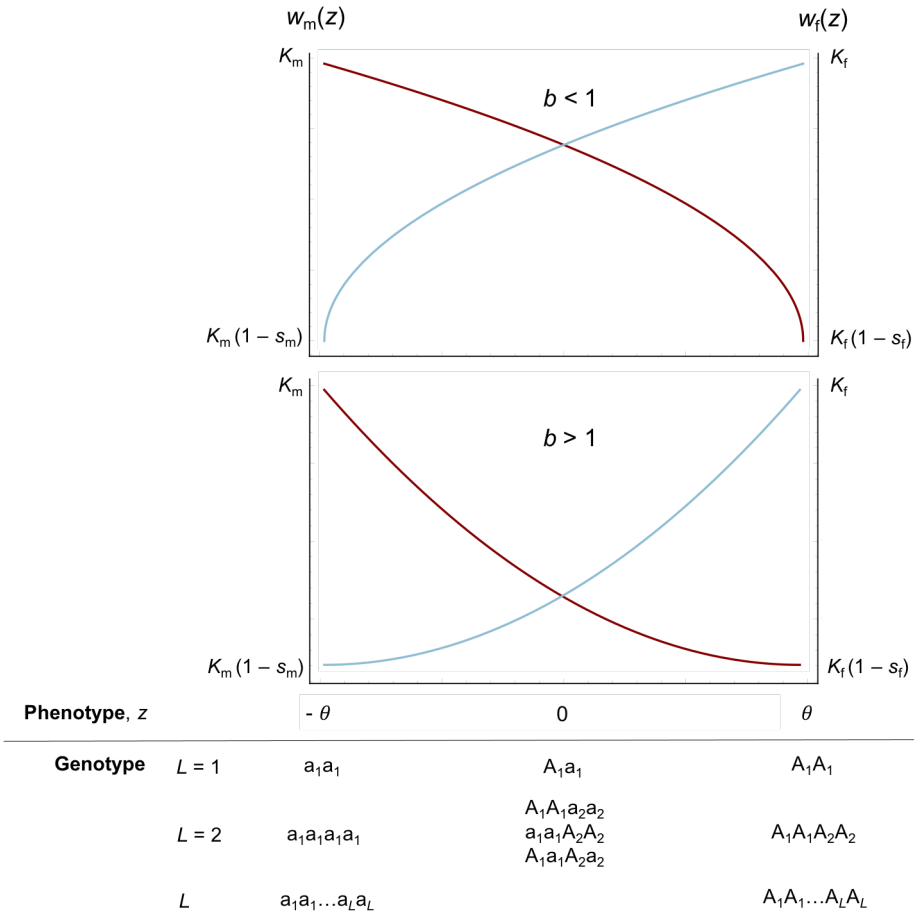

Figure 1: Sex-specific fecundity curves. Male (red curves) and female (blue curves) fecundity as a function of phenotype, z, eq. (1). A male's fecundity is greatest when he expresses the phenotype $z = -\theta$, i.e. he is homozygous for allele a at every locus, while a female's fecundity is maximised when she expresses $z = \theta$, i.e she is homozgous for allele A at all loci (eqs. 2-3). Top and bottom panels show diminishing ($b_m = b_f < 1$) and accelerating ($b_m = b_f > 1$) returns to adaptation in each sex, respectively.

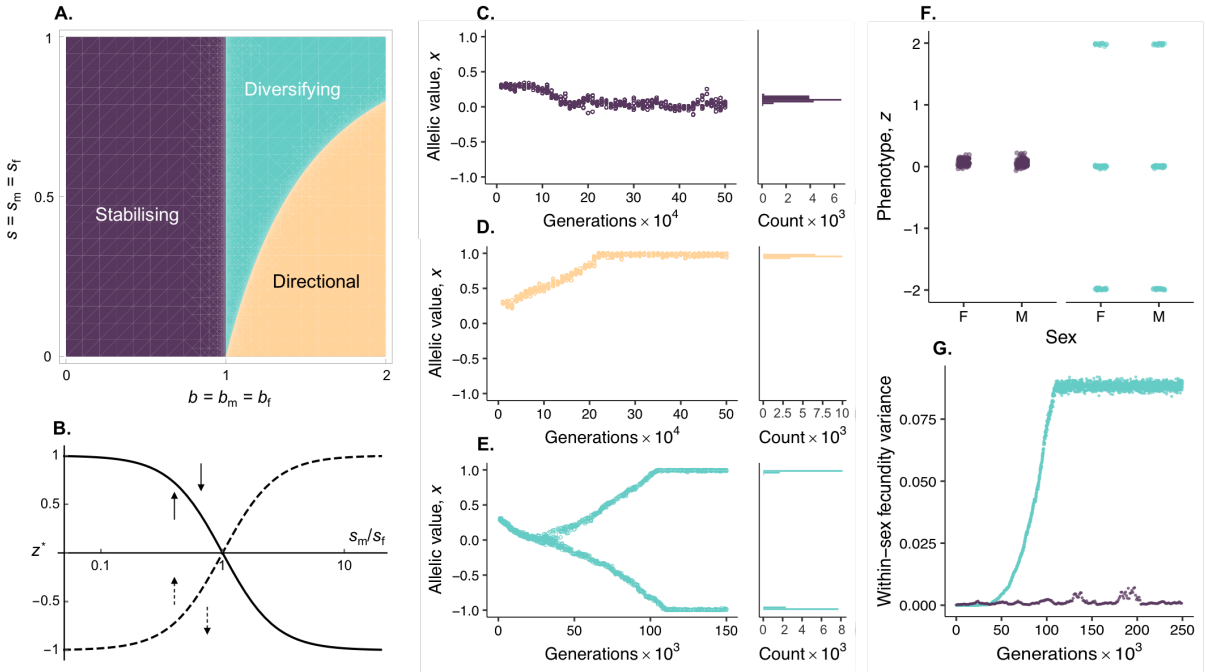

Figure 2: Genetic evolution in a continuum-of-alleles model of sexual antagonism. Panel **A** shows the parameter space leading to each mode of selection (Appendix A for full analysis). Panel **B** shows the singular trait value z^* (eq. 4) as a function of the strength of selection in males versus females s_m/s_f. Solid curve shows z^* when it is an attractor of evolutionary dynamics ("stabilising" and "diversifying" selection), and dashed curve shows z^* when it is a repellor ("directional selection"). Panels **C**-**E** show evolution of allelic values x in a simulation of our continuum-of-alleles model when sexual antagonism leads to stabilising ($s = 0.05, b = 0.5$), directional ($s = 0.05, b = 1.5$) and diversifying ($s = 0.9, b = 1.5$) selection, respectively. In left-hand frame of each panel, dots represent a random sample of 10 alleles from the population at intervals of 10^4 (in C-D) or 10^3 (in E) generations. Right-hand frames show the distribution of all alleles in the final generation. Simulations were initialised with all individuals homozygous for an allelic value of $x = 0.3$, with $\theta = 2$, Appendix A.5 for full simulation procedure. Panel **F** shows shows the phenotypes of a random sample of 50 male and 50 female individuals from a simulation after 2.5×10^5 generations under stabilising (purple dots) and diversifying selection (green dots). Panel **G** shows the average fecundity variance within the sexes ($\mathrm{Var}[w_m(z)]/2 + \mathrm{Var}[w_f(z)]/2$) through time under diversifying (green dots) and stabilising (purple dots) selection. Unless otherwise stated, in all panels the strength of sex-specific selection is equal across males and females, $s = s_m = s_f$, and fecundity landscapes are the same shape, $b = b_m = b_f$.

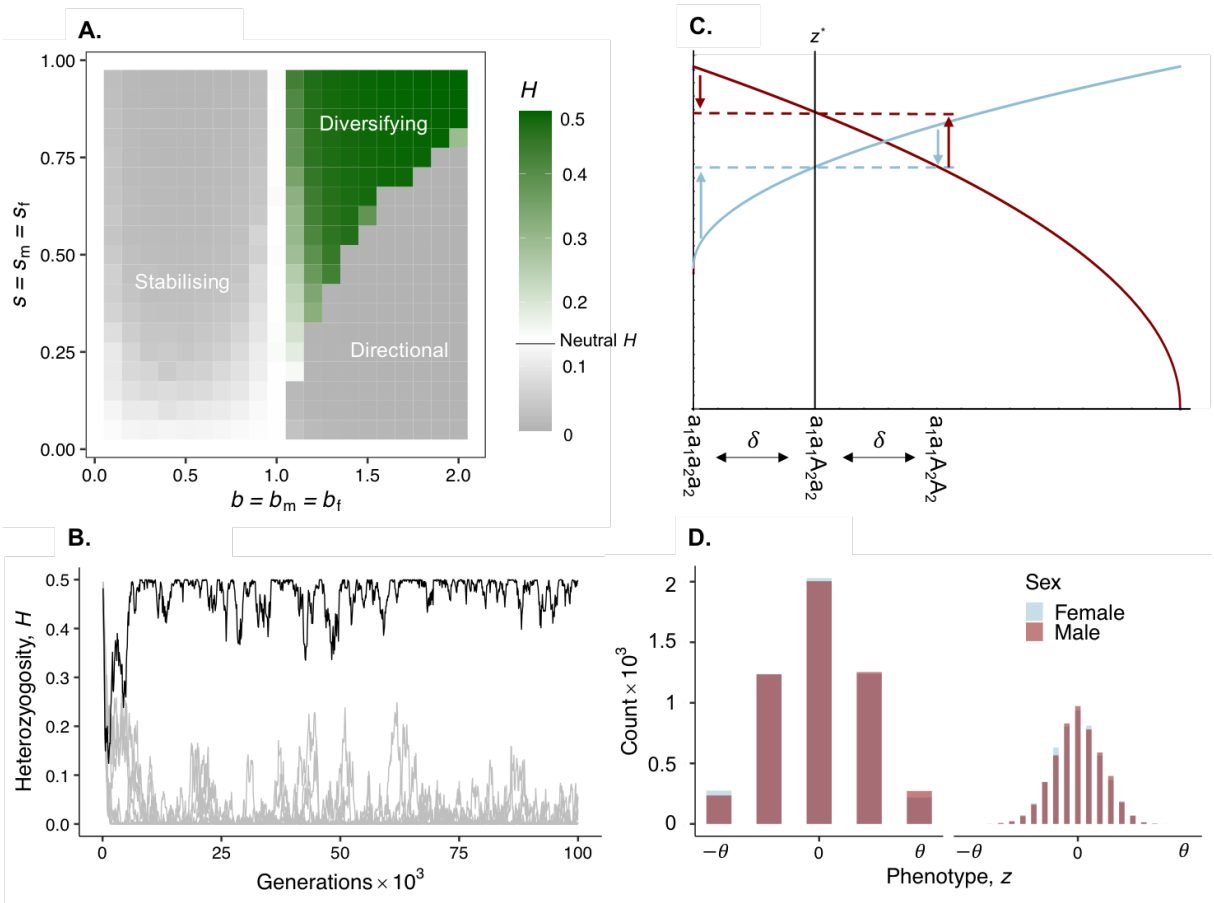

Figure 3: Genetic and phenotypic variation in a polygenic model of sexual antagonism. Panel **A** shows average heterozygosity across loci from polygenic simulations. White, green and grey squares represent average heterozygosity values that are respectively equal, higher, and lower, than that of a neutral locus at mutation-drift balance. Panel **B** shows heterozygosity through time at each individual locus of a polygenic trait ($L = 10$) in a simulation where selection stronger in males than females ($s_m = 0.85 \times 0.3$, $s_f = 0.15 \times 0.3$, $b = 0.5$), black curve shows heterozygosity at the "remainder" locus. Panel **C** shows male (blue curve) and female (red curve) fecundity under stabilising selection ($b < 1$) when sex-specific selection is stronger in males than females ($s_m > s_f$). Dotted horizontal lines show sex-specific fecundity for individuals expressing the optimal phenotype z^* (which here is closer to the male optimum, i.e. $z^* < 0$). Vertical arrows show the fecundity differences between double homozygote genotypes in a two-locus model ($L = 2$) and genotypes that are homozygote for the male beneficial allele at locus 2 (a_2) and heterozygous at locus 1. These reveal dominance reversal at locus 2 (with downward arrows shorter than upward arrows in each sex). Panel **D** shows the distribution of male and female phenotypes of a polygenic trait ($L = 2$ on left and $L = 10$ on right) under diversifying selection ($s_m = s_f = 0.9$, $b = 1.5$) after 10^5 generations of a simulation (note that male and female distributions are mostly indistinguishable). Unless otherwise stated, all panels show results from simulations with $L = 10$ di-allelic loci, Appendix B.3 for full simulation procedures. Other parameters used: $\delta = 1$, $\mu = 10^{-5}$.

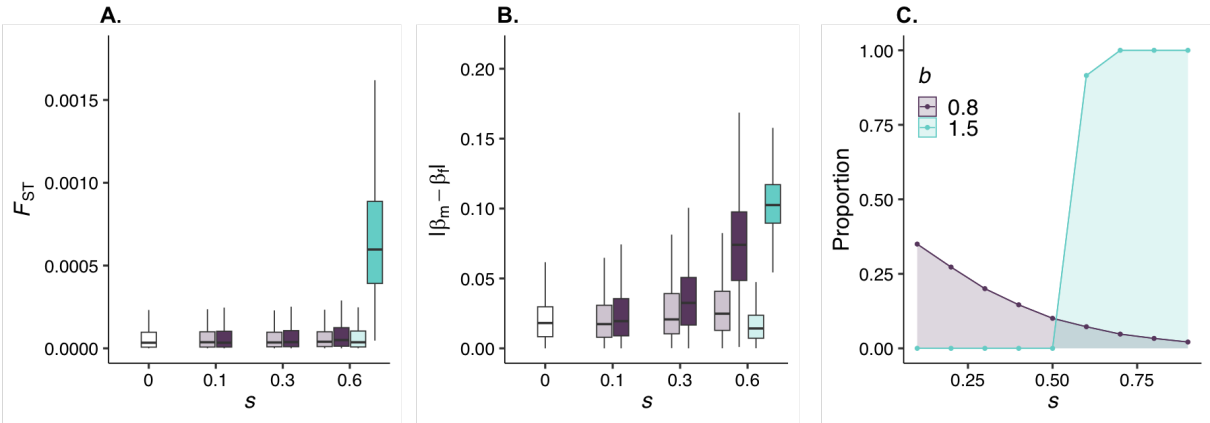

Figure 4: Patterns of allelic variation and fitness associations in polygenic simulations. Panel **A** shows distributions of allelic differentiation (between-sex F_{ST}). Panel **B** shows distributions of absolute sex-differences in the linear regression coefficients of fitness against within-individual allele frequency ($|\beta_{m,k} - \beta_{f,k}|$). In both panels, white boxplots show values for neutral alleles, coloured boxplots show values for sexually antagonistic trait loci (red for $b = 0.8$, green for $b = 1.5$), and translucent coloured boxplots show values for permuted loci as controls (i.e. trait loci where the sex of each individual is randomly assigned). Boxes show the 25th, 50th and 75th quantiles, vertical black lines show the interquartile range. Panel **C** shows the proportion of alleles with minor-allele-frequency greater than 0.05 for loci encoding a trait under sexually antagonistic selection. All panels show results from pooled data of simulations with $L = 10$ di-allelic loci, Appendix D for full simulation procedures and calculations. Other parameters used: $\delta = 1, \mu = 10^{-5}$

Supplementary Figures

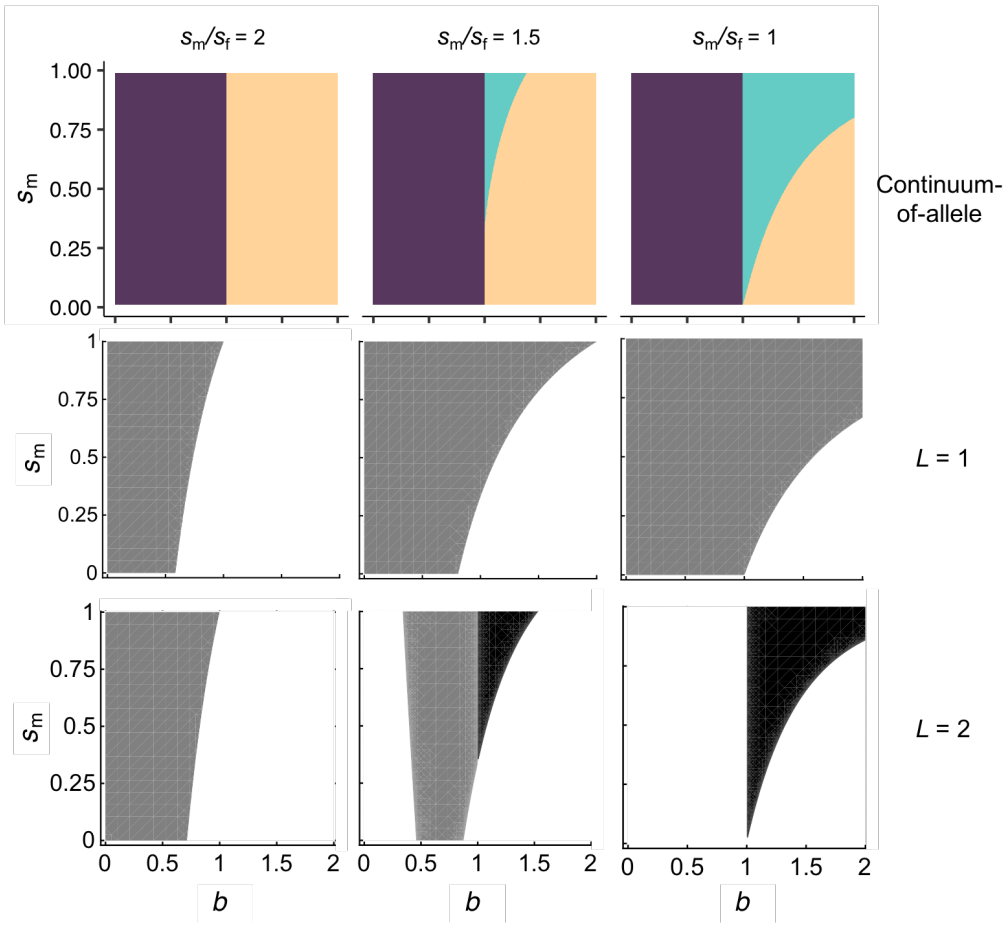

Supplementary Figure 1: The mode of selection and maintenance of genetic variation in the continuum-of-alleles and di-allelic models. Top row panels show parameter space corresponding to stabilising (purple regions), directional (yellow regions), and diversifying (green regions) selection in the continuum-of-alleles model with $\theta = 1$. These plots were generated by numerically solving eq. (A-7) to find singular points and evaluating their stability (Appendix A.4.2 for details). Middle row panels show parameter conditions for polymorphism (grey regions) at a single locus di-allelic ($L = 1, \delta = 1$, see eqs. 3-2). Polymorphism condition corresponds to when inequality (B-19) is satisfied. Bottom row panels show polymorphism space for a trait encoded by two di-allelic loci ($L = 2, \delta = 1$). Grey regions show conditions for polymorphism at one locus (i.e. the other is fixed for one allele), and black region shows conditions for polymorphism at two loci. Grey regions correspond to the conditions where all four haploid genotypes are invadable by another genotype but there is a stable equilibrium where one locus is fixed for one allele, while black regions correspond to parameter space that we found such an equilibrium did not exist (this was done by numerically iterating eq. (B-22)-(B-23), Appendix B.2.2 for details). In all panels, parameter space is in terms of the shape of fecundity curves (b) and the strength of selection in males (s_m) on the x and y axes respectively. Panel columns show plots for different strengths of asymmetry in male and female selection

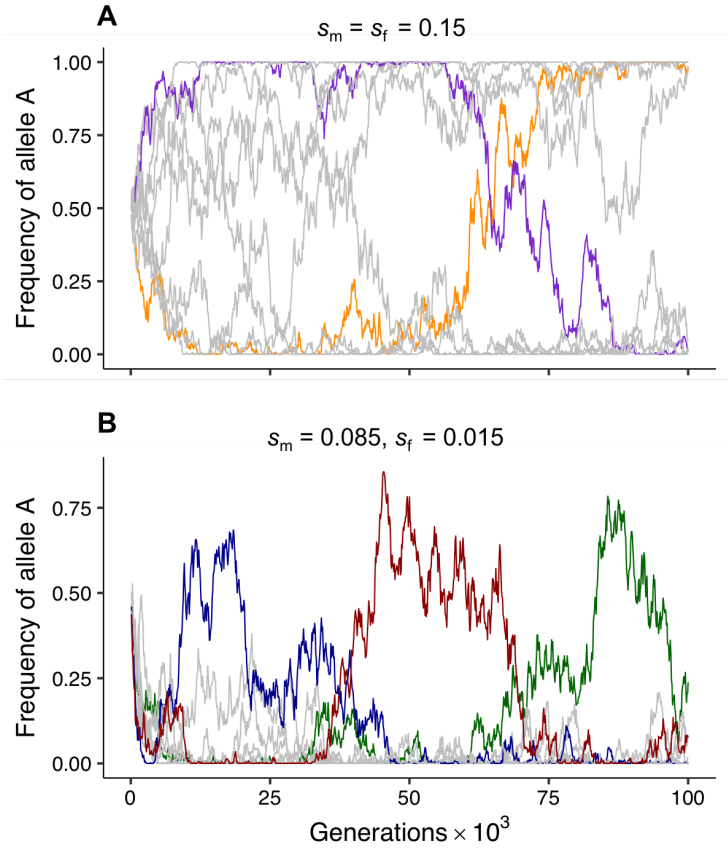

Supplementary Figure 2: Allele frequencies through time under stabilising selection. Lines show frequency of the female-beneficial allele A at each locus through time in a polygenic simulation. **A** shows a case with equal strength selection in both sexes, whereby selection favours the fixation of equal numbers of A and a alleles across loci. Orange and purple lines show an example of two loci that are initially fixed for one allele but exhibit a transient genetic polymorphism by switching to become fixed for the opposing one (due to the combined effects of selection mutation and drift). **B** shows a case of male-biased selection that leads selection to favour polymorphism at a single remainder locus. Dark blue, red, and green, lines showing three different loci that rise to high frequency due to turnover in the identity of the remainder locus owing to mutation and drift. All panels show results from simulations with $L = 10$ di-allelic loci, Appendix B.3 for details. Other parameters used: $b = 0.5, \delta = 1, \mu = 10^{-5}$.

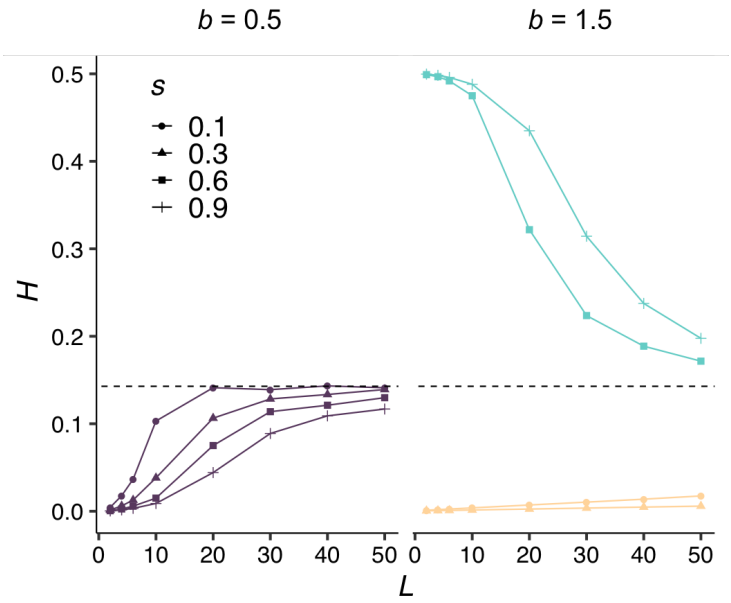

Supplementary Figure 3: Effect of number of loci on heterozygosity in polygenic simulations. Curves show average heterozygosity across L di-allelic loci encoding z. Different curve/point combinations represent different strength of sexually antagonistic selection ($s = s_{\mathrm{m}} = s_{\mathrm{f}} \in [0.1, 0.9]$), left-hand panel shows results for diminishing fecundity curves ($b = 0.5 < 1$) and right-hand panel for accelerating fecundity curves ($b = 1.5 > 1$). Horizontal dashed line shows expected heterozygosity for a neutral locus at mutation-drift balance. Appendix B.3 for simulation details. Other parameters used: $\delta = 1, \mu = 10^{-5}$.

Appendix for "The maintenance of genetic polymorphism in sexually antagonistic traits"

Ewan Flintham[1,2], Vincent Savolainen[2], Sarah Otto[3], Max Reuter[4] and Charles Mullon[1]

[1]Department of Ecology and Evolution, University of Lausanne, 1015 Lausanne, Switzerland

[2]Department of Life Sciences, Georgina Mace Centre for the Living Planet, Silwood Park Campus, Imperial College London, Ascot, SL5 7PY United Kingdom

[3]Department of Zoology, and Biodiversity Research Centre, University of British Columbia, Vancouver, British Columbia, Canada

[4]Department of Genetics, Evolution and Environment, University College London, London, WC1E 6BT United Kingdom

A Continuum-of-alleles model

A.1 Population genetic recursions

As a basis to our analysis of the continuum-of-alleles model, we first consider one locus where a new allele A appearing in a population fixed for allele a. To do so, we write recursion equations for the frequencies of these alleles in adult males and females at generation $t+1$ as a function of their frequencies in generation t. Selection influences allele frequencies through the fecundities of adults carrying the three diploid genotypes AA, Aa, aa and expressing the respective phenotypes z_{AA}, z_{Aa}, z_{aa} (i.e. where z_u is phenotype encoded by genotype $u \in \{\mathrm{AA}, \mathrm{Aa}, \mathrm{aa}\}$). Specifically, the frequency, $p_{v,t+1}$, of A in adults of sex $v \in \{\mathrm{m}, \mathrm{f}\}$ at generation $t+1$ is given by

$$\begin{aligned} p_{\mathrm{m},t+1} &= M(p_{\mathrm{m},t}, p_{\mathrm{f},t}) \\ p_{\mathrm{f},t+1} &= F(p_{\mathrm{m},t}, p_{\mathrm{f},t}), \end{aligned} \tag{A-1}$$

where

$$
\begin{aligned}
M(p_{\mathrm{m},t}, p_{\mathrm{f},t}) &= p_{\mathrm{m},t} p_{\mathrm{f},t} \frac{w_{\mathrm{m}}(z_{\mathrm{AA}})}{\overline{w}_{\mathrm{m},t}} + \frac{1}{2}\big(p_{\mathrm{m},t}(1-p_{\mathrm{f},t}) + (1-p_{\mathrm{m},t})p_{\mathrm{f},t}\big)\frac{w_{\mathrm{m}}(z_{\mathrm{Aa}})}{\overline{w}_{\mathrm{m},t}} \\
F(p_{\mathrm{m},t}, p_{\mathrm{f},t}) &= p_{\mathrm{m},t} p_{\mathrm{f},t} \frac{w_{\mathrm{f}}(z_{\mathrm{AA}})}{\overline{w}_{\mathrm{f},t}} + \frac{1}{2}\big(p_{\mathrm{m},t}(1-p_{\mathrm{f},t}) + (1-p_{\mathrm{m},t})p_{\mathrm{f},t}\big)\frac{w_{\mathrm{f}}(z_{\mathrm{Aa}})}{\overline{w}_{\mathrm{f},t}},
\end{aligned}
\tag{A-2}
$$

and $w_v(z_u)$ is the number of sperm or eggs produced an individual of the genotype $u \in \{\mathrm{AA}, \mathrm{Aa}, \mathrm{aa}\}$ expressing the phenotype z_u in sex v (eq. 1), and $\overline{w}_{\mathrm{m},t} = p_{\mathrm{m},t} p_{\mathrm{f},t} w_{\mathrm{m}}(z_{\mathrm{AA}}) + \big(p_{\mathrm{m},t}(1-p_{\mathrm{f},t}) + (1-p_{\mathrm{m},t})p_{\mathrm{f},t}\big) w_{\mathrm{m}}(z_{\mathrm{Aa}}) + (1-p_{\mathrm{m},t})(1-p_{\mathrm{f},t}) w_{\mathrm{m}}(z_{\mathrm{aa}})$ and $\overline{w}_{\mathrm{f},t} = p_{\mathrm{m},t} p_{\mathrm{f},t} w_{\mathrm{f}}(z_{\mathrm{AA}}) + \big(p_{\mathrm{m},t}(1-p_{\mathrm{f},t}) + (1-p_{\mathrm{m},t})p_{\mathrm{f},t}\big) w_{\mathrm{f}}(z_{\mathrm{Aa}}) + (1-p_{\mathrm{m},t})(1-p_{\mathrm{f},t}) w_{\mathrm{f}}(z_{\mathrm{aa}})$ are mean male and female fecundities at generation t, respectively.

Allele A can invade when rare (i.e. when $p_{\mathrm{m},t} = p_{\mathrm{f},t}$ are small) when the leading eigenvalue, $\lambda(0)$, of the Jacobian matrix,

$$
\mathrm{J}(0) = \begin{pmatrix} \dfrac{\partial M(p_{\mathrm{m},t}, p_{\mathrm{f},t})}{\partial p_{\mathrm{m},t}} & \dfrac{\partial M(p_{\mathrm{m},t}, p_{\mathrm{f},t})}{\partial p_{\mathrm{f},t}} \\ \dfrac{\partial F(p_{\mathrm{m},t}, p_{\mathrm{f},t})}{\partial p_{\mathrm{m},t}} & \dfrac{\partial F(p_{\mathrm{m},t}, p_{\mathrm{f},t})}{\partial p_{\mathrm{f},t}} \end{pmatrix}_{p_{\mathrm{m},t}=p_{\mathrm{f},t}=0},
\tag{A-3}
$$

is greater than unity ($\lambda(0) > 1$). This leading eigenvalue equals:

$$
\lambda(0) = \frac{1}{2}\frac{w_{\mathrm{m}}(z_{\mathrm{Aa}})}{w_{\mathrm{m}}(z_{\mathrm{aa}})} + \frac{1}{2}\frac{w_{\mathrm{f}}(z_{\mathrm{Aa}})}{w_{\mathrm{f}}(z_{\mathrm{aa}})},
\tag{A-4}
$$

for any fitness functions in males and females, both for strong and weak selection, as long as the resident population consists only of a single allele, a.

A.2 Invasion fitness and adaptive dynamics

Here, we analyse evolutionary dynamics under the continuum-of-alleles model in diploids, following e.g. [1]. As a basis to such an analysis, we need the invasion fitness (i.e. geometric growth rate), $W(x_\bullet, x)$, of a rare mutant allele that encodes an additive phenotypic effect $x_\bullet$ in a population that is otherwise fixed for an allele encoding an effect x. From the above (Appendix A.1), invasion of such a mutant allele is determined by eq. (A-4) with mutant heterozygote phenotype $z_{\mathrm{Aa}} = x_\bullet + x$ and resident homozygote phenotype $z_{\mathrm{aa}} = 2x$. Accordingly, invasion fitness is given by,

$$
W(x_\bullet, x) = \frac{1}{2}\frac{w_{\mathrm{m}}(x_\bullet + x)}{w_{\mathrm{m}}(2x)} + \frac{1}{2}\frac{w_{\mathrm{f}}(x_\bullet + x)}{w_{\mathrm{f}}(2x)}.
\tag{A-5}
$$

Given a small change in phenotype (so that $x_\bullet$ is close to x), the selection gradient determines the form of directional selection:

$$
S(x) = \left.\frac{\partial W(x_\bullet, x)}{\partial x_\bullet}\right|_{x_\bullet = x},
\tag{A-6}
$$

i.e. $S(x)$ indicates whether in a population fixed for x, selection favours an increase in allelic value when $S(x) > 0$ or a decrease when $S(x) < 0$. A singular allelic value x^* is such that when expressed by the whole population,

there is no directional selection, i.e. such that

$$S(x^*) = 0. \tag{A-7}$$

Whether evolutionary dynamics converge to such a singularity depends on the sign of

$$S'(x^*) = \left.\frac{dS(x)}{dx}\right|_{x=x^*}. \tag{A-8}$$

If $S'(x^*) < 0$, then x^* is an attractor of evolutionary dynamics, i.e. it is convergence stable [2], so that owing to directional selection and mutational input, the population will gradually converge to x^* and thus express the phenotype $z^* = 2x^*$. By contrast, if $S'(x^*) > 0$, then x^* is a repellor of evolutionary dynamics so that the population will gradually converge away from x^*.

If a population converges to a singular allelic value x^*, evolutionary dynamics are then determined by quadratic selection, i.e. by the second order fitness effect, which is given by

$$H(x^*) = \left.\frac{\partial^2 W(x_\bullet, x)}{\partial x_\bullet^2}\right|_{x_\bullet = x = x^*}. \tag{A-9}$$

When $H(x^*) < 0$, selection is stabilising [3], selecting against any mutant that deviates from x^*, i.e. x^* is uninvadable [4]. When $H(x^*) > 0$, selection is diversifying (or negatively frequency-dependent and disruptive), favouring the emergence of polymorphism. The distribution of allelic values in the population thus goes from being unimodal to bimodal in a process referred to as evolutionary branching [5, 6].

A.3 Equal selection in males and females

We now consider the fitness function eq. (1), assuming initially that selection is the same strength in both sexes ($s = s_\mathrm{m} = s_\mathrm{f}$) as this lends itself better to mathematical scrutiny. Plugging eq. (1) into eq. (A-5) and setting $s = s_\mathrm{m} = s_\mathrm{f}$, we find that invasion fitness reduces to

$$W(x_\bullet, x) = \frac{1}{2}\cdot\frac{1 - s\left[1 + 2^{-b}\left(\frac{\theta - x - x_\bullet}{\theta}\right)^b\right]}{1 - s\left[1 + \left(\frac{1}{2} - \frac{x}{\theta}\right)^b\right]} + \frac{1}{2}\cdot\frac{1 - s\left[1 + 2^{-b}\left(\frac{\theta + x + x_\bullet}{\theta}\right)^b\right]}{1 - s\left[1 + \left(\frac{1}{2} + \frac{x}{\theta}\right)^b\right]}. \tag{A-10}$$

In turn, plugging eq. (A-10) into (A-6) we obtain the selection gradient

$$S(x) = \frac{1}{2}bs\left[\frac{1}{s + (1-s)\left(\frac{1}{2} + \frac{x}{\theta}\right)^{-b}(2x - \theta)} + \frac{1}{s + (1-s)\left(\frac{1}{2} - \frac{x}{\theta}\right)^{-b}(2x + \theta)}\right], \tag{A-11}$$

from which it can be seen that $x^* = 0$ is always a singular point (i.e. $S(0) = 0$). Substituting eq. (A-11) into eq. (A-11), and evaluating the result at $x^* = 0$ yields

$$S'(0) = \frac{2sb\left[2^b(b-1)(1-s) - s\right]}{\left[2^b + s(1 - 2^b)\right]^2}. \tag{A-12}$$

This show that $S'(0) < 0$ and $x^* = 0$ is an attractor of selection, either when

$$b < 1 \tag{A-13}$$

(i.e. fecundity curves are diminishing), or when

$$\begin{cases} b > 1 \\ s > \dfrac{1}{1 + \frac{1}{2^b(b-1)}} \end{cases} \tag{A-14}$$

(i.e. curves are accelerating and selection is sufficiently strong). Otherwise, $S'(0) > 0$ and $x^* = 0$ is a repellor, with selection being directional towards $x = \theta$ if the population initially is fixed for an allelic value above 0 ($x > 0$) or $x = -\theta$ if initially below 0 ($x < 0$).

Plugging eq. (A-10) into (A-9) and evaluating the result at $x^* = 0$ gives us

$$H(0) = \frac{sb(b-1)}{2^b(1-s)+s}. \tag{A-15}$$

This shows that whenever $b < 1$, the singular trait value $x^* = 0$ is under stabilising selection (as $H(0) < 0$). Otherwise, $H(0) > 0$ so that if eq. (A-14) also holds, $x^* = 0$ is an evolutionary branching point where selection is diversifying. These results are summarised in Fig. 2A.

A.4 Asymmetric selection

The case of asymmetric selection between the sexes ($s_\mathrm{m} \neq s_\mathrm{f}$) is more complicated. To gain some analytical insights, we first assume that selection is weak (i.e. that s_m and s_f are small).

A.4.1 Weak selection

Substituting main text eq. (1) into eq. (A-5), mutant fitness can be expressed

$$W(x_\bullet, x) = \frac{1}{4}\left[2 - 2^{-b}s_\mathrm{m}\left(\left(1-\frac{2x}{\theta}\right)^b - \left(\frac{\theta - x_\bullet - x}{\theta}\right)^{b_\mathrm{m}}\right) - 2^{-b}s_\mathrm{f}\left(\left(1+\frac{2x}{\theta}\right)^b - \left(\frac{\theta + x_\bullet + x}{\theta}\right)^b\right)\right] + \mathcal{O}(\epsilon^2), \tag{A-16}$$

where $s_\mathrm{m} \sim \mathcal{O}(\epsilon)$, $s_\mathrm{f} \sim \mathcal{O}(\epsilon)$ and $0 < \epsilon \ll 1$ is a small parameter. Plugging eq. (A-16) into eq. (A-6), we then find the singular allelic value

$$x^* = \theta \frac{1 - (s_\mathrm{m}/s_\mathrm{f})^{1/(1-b)}}{2\left(1 + (s_\mathrm{m}/s_\mathrm{f})^{1/(1-b)}\right)} + \mathcal{O}(\epsilon^2). \tag{A-17}$$

The equilibrium phenotype, which is given by $2x^*$, is shown in main text eq. (4).

The convergence stability of a singular strategy x^* is considered for general fitness functions in Appendix sec-

tion C.4.1. Here, we apply these results, assuming weak selection (so that the terms in curly braces in eq. C-36 are negligible). Whenever the curvature for the male and female fitness function are both negative (i.e. $b < 1$), the singular point will be convergence stable ($S'(x^*) < 0$) and subject to stabilizing selection ($H(x^*) < 0$, see eq. C-37). Conversely, when the curvature for the male and female fitness functions are both positive (i.e. $b > 1$), the singular point will be a repellor and not convergence stable ($S'(x^*) > 0$, $H(x^*) > 0$). Thus, with weak selection, there is either stabilising selection ($b < 1$) or directional selection ($b > 1$), but never diversifying selection (see also eq. C-38 for a more general argument).

A.4.2 Arbitrarily strong selection

We analysed the general case ($s_\mathrm{m} \neq s_\mathrm{f}$) using a numerical approach. Specifically, we first solved numerically eq. (A-7) for x^* and analysed its stability by evaluating eqs. (A-8)-(A-9). We did this for a range of parameter values within $s_\mathrm{m} \in [0,1]$, $b \in [0,2]$ and $\alpha \in [0,1]$ where $s_\mathrm{f} = \alpha s_\mathrm{m}$.

Our results are summarized in the top row panels of Appendix Fig. 1. These show that selection is stabilising forx^* whenever fecundity curves are diminishing ($b < 1$, Appendix Fig. 1 purple region), that selection is diversifying when selection in males and females is strong and of similar intensity (Appendix Fig. 1 green region), and that otherwise selection is directional towards $x = -\theta$ or $x = \theta$ depending on whether the population is initially below or above x^* (Appendix Fig. 1 orange region).

A.5 Simulations

We ran individual-based simulations of the continuum-of-alleles model using SLiM 4 [7], whose results are presented in Fig. 2. Following the life cycle described in section 2, we consider a diploid population of 5'000 adult males and 5'000 adult females with non-overlapping generations. Each individual is characterised by the two allelic values it carries. At the beginning of the next generation, say $t+1$, 5000 male and 5000 female offspring are created, with the mother and father of each offspring being sampled from the adult females and males at generation t. Sampling is performed with replacement according to a multinomial distribution where the weighting on each male and female individual is according to their fecundity

$$\begin{aligned} w_\mathrm{m}(z) &= (1 - s_\mathrm{m}) + s_\mathrm{m}\left(\frac{\theta - z}{2\theta}\right)^{b_\mathrm{m}} \\ w_\mathrm{f}(z) &= (1 - s_\mathrm{f}) + s_\mathrm{f}\left(\frac{\theta + z}{2\theta}\right)^{b_\mathrm{f}}, \end{aligned} \tag{A-18}$$

(eq. 1), where z is the sum of the two allelic values carried. Each parent transmits one of the copies it carries, each with equal probability (i.e. no segregation bias). Mutations occur at a per-locus rate μ with a new mutation adding a deviate sampled from a Normal distribution $N(0, 0.005)$ onto the existing allelic value at the mutating gene. After sampling, adults are removed from the simulations, juveniles become adults and the new generation begins.

B Di-allelic model

In this appendix, we model trait z as being encoded by L di-allelic loci, with a male- and female-beneficial allele at each locus (when $L > 1$ this is the polygenic model described in the main text). We analyse this model mathematically for the cases $L = 1$ and $L = 2$ and with simulations for $L > 2$. Our results show that polymorphism is more easily maintained where genetic constraints are extremely strong, that is where the trait is underlain by very few loci and thus where there are few alleles available.

B.1 Dynamics at a single locus

B.1.1 Reciprocal invasion

To connect to classical results [8], we first consider a trait encoded by a single di-allelic locus ($L = 1$), i.e. at which the alleles A_1 and a_1 (denoted A and a in this subsection) segregate. We assume that these alleles span the phenotypic range, so that the three diploid genotypes AA, Aa, aa express the phenotypes $z_{AA} = \theta$, $z_{Aa} = 0$, $z_{aa} = -\theta$. The recursion equations describing the change in frequency of these two alleles are given by eq. (A-1). Balancing selection at a locus occurs whenever each allele (A and a) can be invaded by the other (reciprocal invasion). First, allele A can invade a population fixed for a (i.e. where $p_{m,t} = p_{f,t} = 0$) when the leading eigenvalue, $\lambda(0)$, of the Jacobian matrix J(0) given by eq. (A-3) is greater than one. Similarly, allele a can invade a population fixed for A when the leading eigenvalue, $\lambda(1)$, of the Jacobian matrix J(1) is greater than one, where J(1) is given by the matrix eq. (A-3) evaluated now at $p_{m,t} = p_{f,t} = 1$.

Plugging eq. (1) into eq. (A-1) and eq. (A-1) into J(0) and J(1), we obtain a single condition for $\lambda(0) > 1$ and $\lambda(1) > 1$ to be satisfied,

$$\frac{2^b - 1}{1 + (2^b - 1)s_f} < s_m / s_f < \frac{1}{(2^b - 1)(1 - s_f)} \tag{B-19}$$

which corresponds to a classical condition for a protected polymorphism at a single sexually antagonistic locus (eq. 7 in [8] and eq. 3 in [9] where $h_m = h_f = 1 - 2^{-b}$). Inequality (B-19) is satisfied most readily when $b < 1$, as this favours an intermediate value of z that is encoded by the heterozygote Aa, i.e. there is dominance reversal for fitness (Supplementary Fig. 1 middle row panels). This result differs substantially from the continuum-of alleles model (Supplementary Fig. 1 compare top and middle row panels), where polymorphism is never maintained with $b < 1$, and reflects the fact that we now constrain the system to have only two alleles, which straddle $x^* = 0$ (with phenotypes θ for AA and $-\theta$ for aa).

Polymorphism may also be maintained when $b > 1$ if selection is strong (s_m and s_m both large and similar), although the conditions for this to occur are more permissive than in the continuum-of-alleles case (Supplementary Fig. 1 compare top and middle row panels). This is because the single locus model considers the segregation of two already highly differentiated alleles, A and a (rather than the gradual evolution of allelic values

through mutations of small effect in the continuum-of-alleles model), which more easily allows for reciprocal invasibility.

B.2 Dynamics at two loci

Second we consider when z is determined by two di-allelic loci (locus 1 where alleles a_1, A_1 segregate, and locus 2 where alleles a_2, A_2 segregate).

B.2.1 Recursions

To characterise allele frequency change at two loci, we now track the dynamics of the haploid male and female gamete genotypes [10–13] rather than adult allele frequencies. We denote the sex-specific frequencies of each gametic genotype in generation t (before syngamy) as $m_{1,t}, m_{2,t}, m_{3,t}, m_{4,t}$ in male gametes, and $f_{1,t}, f_{2,t}, f_{3,t}, f_{4,t}$ in female gametes, for the genotypes A_1A_2, A_1a_2, a_1A_2, and a_1a_2 respectively (where $\sum_{i=1}^{4} m_{i,t} = \sum_{i=1}^{4} f_{i,t} = 1$). Meanwhile, adult genotypes at generation t are denoted $g^{\mathrm{m}}_{ij,t}$ in males and $g^{\mathrm{f}}_{ij,t}$ in females, where $i \in \{1,2,3,4\}$ and $j \in \{1,2,3,4\}$ respectively refer to the different paternally and maternally inherited haploid genotypes. Following the lifecycle in section 2, adult genotype frequencies in each sex depend on the sex-specific gametic frequencies according to

$$\begin{aligned} g^{\mathrm{m}}_{ij,t} &= f_{i,t} m_{j,t} \\ g^{\mathrm{f}}_{ij,t} &= f_{i,t} m_{j,t} \end{aligned} \tag{B-20}$$

in males and females, and from eqs. (2)-(3), the adult phenotypes are

$$\begin{aligned} z_{11} &= 4\delta \\ z_{12} &= z_{13} = 3\delta \\ z_{14} &= z_{22} = z_{22} = z_{23} = z_{33} = 0 \\ z_{24} &= z_{34} = -3\delta \\ z_{44} &= -4\delta, \end{aligned} \tag{B-21}$$

where $z_{ij} = z_{ji}$ is the phenotype encoded by adult diploid genotype ij. We can therefore write recursion equations for the male and female gametes as

$$\begin{aligned} m_{1,t+1} &= M_1(\mathbf{g}^{\mathrm{m}}_t) \\ m_{2,t+1} &= M_2(\mathbf{g}^{\mathrm{m}}_t) \\ m_{3,t+1} &= M_3(\mathbf{g}^{\mathrm{m}}_t) \\ m_{4,t+1} &= M_4(\mathbf{g}^{\mathrm{m}}_t), \end{aligned} \tag{B-22}$$

and

$$
\begin{aligned}
f_{1,t+1} &= F_1(\mathbf{g}_t^{\mathrm{f}}) \\
f_{2,t+1} &= F_2(\mathbf{g}_t^{\mathrm{f}}) \\
f_{3,t+1} &= F_3(\mathbf{g}_t^{\mathrm{f}}) \\
f_{4,t+1} &= F_4(\mathbf{g}_t^{\mathrm{f}}),
\end{aligned}
\tag{B-23}
$$

respectively, where $\mathbf{g}_t^{\mathrm{m}} = (g_{11,t}^{\mathrm{m}}, \ldots, g_{44,t}^{\mathrm{m}})$ and $\mathbf{g}_t^{\mathrm{f}} = (g_{11,t}^{\mathrm{f}}, \ldots, g_{44,t}^{\mathrm{f}})$ and where the functions $M_1(\mathbf{g}_t^{\mathrm{m}}), M_2(\mathbf{g}_t^{\mathrm{m}}), M_3(\mathbf{g}_t^{\mathrm{m}}), M_4(\mathbf{g}_t^{\mathrm{m}})$ and $F_1(\mathbf{g}_t^{\mathrm{f}}), F_2(\mathbf{g}_t^{\mathrm{f}}), F_3(\mathbf{g}_t^{\mathrm{f}}), F_4(\mathbf{g}_t^{\mathrm{f}})$ are

$$
\begin{aligned}
M_1(\mathbf{g}_t^{\mathrm{m}}) &= \frac{w_{\mathrm{m}}(z_{11})}{\overline{w}_{\mathrm{m},t}} g_{11,t}^{\mathrm{m}} + \frac{1}{2}\Big[\frac{w_{\mathrm{m}}(z_{12})}{\overline{w}_{\mathrm{m},t}}(g_{12,t}^{\mathrm{m}} + g_{21,t}^{\mathrm{m}}) + \frac{w_{\mathrm{m}}(z_{13})}{\overline{w}_{\mathrm{m},t}}(g_{13,t}^{\mathrm{m}} + g_{31,t}^{\mathrm{m}}) + (1-r)\frac{w_{\mathrm{m}}(z_{14})}{\overline{w}_{\mathrm{m},t}}(g_{14,t}^{\mathrm{m}} + g_{41,t}^{\mathrm{m}}) + \\
&\qquad r\frac{w_{\mathrm{m}}(z_{23})}{\overline{w}_{\mathrm{m},t}}(g_{23,t}^{\mathrm{m}} + g_{32,t}^{\mathrm{m}})\Big] \\
M_2(\mathbf{g}_t^{\mathrm{m}}) &= \frac{w_{\mathrm{m}}(z_{22})}{\overline{w}_{\mathrm{m},t}} g_{22,t}^{\mathrm{m}} + \frac{1}{2}\Big[\frac{w_{\mathrm{m}}(z_{12})}{\overline{w}_{\mathrm{m},t}}(g_{12,t}^{\mathrm{m}} + g_{21,t}^{\mathrm{m}}) + \frac{w_{\mathrm{m}}(z_{24})}{\overline{w}_{\mathrm{m},t}}(g_{24,t}^{\mathrm{m}} + g_{42,t}^{\mathrm{m}}) + (1-r)\frac{w_{\mathrm{m}}(z_{23})}{\overline{w}_{\mathrm{m},t}}(g_{23,t}^{\mathrm{m}} + g_{32,t}^{\mathrm{m}}) + \\
&\qquad r\frac{w_{\mathrm{m}}(z_{14})}{\overline{w}_{\mathrm{m},t}}(g_{14,t}^{\mathrm{m}} + g_{41,t}^{\mathrm{m}})\Big] \\
M_3(\mathbf{g}_t^{\mathrm{m}}) &= \frac{w_{\mathrm{m}}(z_{33})}{\overline{w}_{\mathrm{m},t}} g_{33,t}^{\mathrm{m}} + \frac{1}{2}\Big[\frac{w_{\mathrm{m}}(z_{13})}{\overline{w}_{\mathrm{m},t}}(g_{13,t}^{\mathrm{m}} + g_{31,t}^{\mathrm{m}}) + \frac{w_{\mathrm{m}}(z_{34})}{\overline{w}_{\mathrm{m},t}}(g_{34,t}^{\mathrm{m}} + g_{43,t}^{\mathrm{m}}) + (1-r)\frac{w_{\mathrm{m}}(z_{23})}{\overline{w}_{\mathrm{m},t}}(g_{23,t}^{\mathrm{m}} + g_{32,t}^{\mathrm{m}}) + \\
&\qquad r\frac{w_{\mathrm{m}}(z_{14})}{\overline{w}_{\mathrm{m},t}}(g_{14,t}^{\mathrm{m}} + g_{41,t}^{\mathrm{m}})\Big] \\
M_4(\mathbf{g}_t^{\mathrm{m}}) &= \frac{w_{\mathrm{m}}(z_{44})}{\overline{w}_{\mathrm{m},t}} g_{44,t}^{\mathrm{m}} + \frac{1}{2}\Big[\frac{w_{\mathrm{m}}(z_{24})}{\overline{w}_{\mathrm{m},t}}(g_{24,t}^{\mathrm{m}} + g_{42,t}^{\mathrm{m}}) + \frac{w_{\mathrm{m}}(z_{34})}{\overline{w}_{\mathrm{m},t}}(g_{34,t}^{\mathrm{m}} + g_{43,t}^{\mathrm{m}}) + (1-r)\frac{w_{\mathrm{m}}(z_{14})}{\overline{w}_{\mathrm{m},t}}(g_{14,t}^{\mathrm{m}} + g_{41,t}^{\mathrm{m}}) + \\
&\qquad r\frac{w_{\mathrm{m}}(z_{23})}{\overline{w}_{\mathrm{m},t}}(g_{23,t}^{\mathrm{m}} + g_{32,t}^{\mathrm{m}})\Big],
\end{aligned}
\tag{B-24}
$$

and

$$
\begin{aligned}
F_1(\mathbf{g}_t^{\mathrm{f}}) &= \frac{w_{\mathrm{f}}(z_{11})}{\overline{w}_{\mathrm{f},t}} g_{11,t}^{\mathrm{f}} + \frac{1}{2}\Big[\frac{w_{\mathrm{f}}(z_{12})}{\overline{w}_{\mathrm{f},t}}(g_{12,t}^{\mathrm{f}} + g_{21,t}^{\mathrm{f}}) + \frac{w_{\mathrm{f}}(z_{13})}{\overline{w}_{\mathrm{f},t}}(g_{13,t}^{\mathrm{f}} + g_{31,t}^{\mathrm{f}}) + (1-r)\frac{w_{\mathrm{f}}(z_{14})}{\overline{w}_{\mathrm{f},t}}(g_{14,t}^{\mathrm{f}} + g_{41,t}^{\mathrm{f}}) + \\
&\qquad r\frac{w_{\mathrm{f}}(z_{23})}{\overline{w}_{\mathrm{f},t}}(g_{23,t}^{\mathrm{f}} + g_{32,t}^{\mathrm{f}})\Big] \\
F_2(\mathbf{g}_t^{\mathrm{f}}) &= \frac{w_{\mathrm{f}}(z_{22})}{\overline{w}_{\mathrm{f},t}} g_{22,t}^{\mathrm{f}} + \frac{1}{2}\Big[\frac{w_{\mathrm{f}}(z_{12})}{\overline{w}_{\mathrm{f},t}}(g_{12,t}^{\mathrm{f}} + g_{21,t}^{\mathrm{f}}) + \frac{w_{\mathrm{f}}(z_{24})}{\overline{w}_{\mathrm{f},t}}(g_{24,t}^{\mathrm{f}} + g_{42,t}^{\mathrm{f}}) + (1-r)\frac{w_{\mathrm{f}}(z_{23})}{\overline{w}_{\mathrm{f},t}}(g_{23,t}^{\mathrm{f}} + g_{32,t}^{\mathrm{f}}) + \\
&\qquad r\frac{w_{\mathrm{f}}(z_{14})}{\overline{w}_{\mathrm{f},t}}(g_{14,t}^{\mathrm{f}} + g_{41,t}^{\mathrm{f}})\Big] \\
F_3(\mathbf{g}_t^{\mathrm{f}}) &= \frac{w_{\mathrm{f}}(z_{33})}{\overline{w}_{\mathrm{f},t}} g_{33,t}^{\mathrm{f}} + \frac{1}{2}\Big[\frac{w_{\mathrm{f}}(z_{13})}{\overline{w}_{\mathrm{f},t}}(g_{13,t}^{\mathrm{f}} + g_{31,t}^{\mathrm{f}}) + \frac{w_{\mathrm{f}}(z_{34})}{\overline{w}_{\mathrm{f},t}}(g_{34,t}^{\mathrm{f}} + g_{43,t}^{\mathrm{f}}) + (1-r)\frac{w_{\mathrm{f}}(z_{23})}{\overline{w}_{\mathrm{f},t}}(g_{23,t}^{\mathrm{f}} + g_{32,t}^{\mathrm{f}}) + \\
&\qquad r\frac{w_{\mathrm{f}}(z_{14})}{\overline{w}_{\mathrm{f},t}}(g_{14,t}^{\mathrm{f}} + g_{41,t}^{\mathrm{f}})\Big] \\
F_4(\mathbf{g}_t^{\mathrm{f}}) &= \frac{w_{\mathrm{f}}(z_{44})}{\overline{w}_{\mathrm{f},t}} g_{44,t}^{\mathrm{f}} + \frac{1}{2}\Big[\frac{w_{\mathrm{f}}(z_{24})}{\overline{w}_{\mathrm{f},t}}(g_{24,t}^{\mathrm{f}} + g_{42,t}^{\mathrm{f}}) + \frac{w_{\mathrm{f}}(z_{34})}{\overline{w}_{\mathrm{f},t}}(g_{34,t}^{\mathrm{f}} + g_{43,t}^{\mathrm{f}}) + (1-r)\frac{w_{\mathrm{f}}(z_{14})}{\overline{w}_{\mathrm{f},t}}(g_{14,t}^{\mathrm{f}} + g_{41,t}^{\mathrm{f}}) + \\
&\qquad r\frac{w_{\mathrm{f}}(z_{23})}{\overline{w}_{\mathrm{f},t}}(g_{23,t}^{\mathrm{f}} + g_{32,t}^{\mathrm{f}})\Big],
\end{aligned}
\tag{B-25}
$$

where r is the recombination rate between the two loci, $w_u(z_{ij})/\overline{w}_u$ is the relative fecundity of a diploid adult with genotype ij or ji in sex u, and $\overline{w}_{u,t} = \sum_{i=1}^{4}\sum_{j=1}^{4} w_u(z_{ij})(g^u_{ij,t} + g^u_{ji,t})$ is the sex-specific mean fecundity in the population at generation t.

B.2.2 Analysis

We focus here on a pair of unlinked loci ($r = 1/2$; linkage is considered in Appendix C.3). With $L = 2$, a necessary condition for balancing selection to occur at either locus is that all four gamete genotypes can be invaded by at least one other genotype when common, that is, when the equilibrium frequencies $m_{1,t} = f_{1,t} = 1, m_{2,t} = f_{2,t} = 1, m_{3,t} = f_{3,t} = 1$ and $m_{4,t} = f_{4,t} = 1$ are all unstable. For compactness, let us collect haploid genotype frequencies into a vector $\mathbf{n}_t = (m_{1,t}, m_{2,t}, m_{3,t}, m_{4,t}, f_{1,t}, f_{2,t}, f_{3,t}, f_{4,t})$. Following this lexicographic order, can write the four fixation states as $\hat{\mathbf{n}}_1 = (1,0,0,0,1,0,0,0)$, $\hat{\mathbf{n}}_2 = (0,1,0,0,0,1,0,0)$, $\hat{\mathbf{n}}_3 = (0,0,1,0,,0,1,0)$, $\hat{\mathbf{n}}_4 = (0,0,0,1,0,0,0,1)$. A given fixation state $\hat{\mathbf{n}}_i$ is unstable when the leading eigenvalue, $\lambda(\hat{\mathbf{n}}_i)$, of the Jacobian matrix

$$\mathrm{J}(\hat{\mathbf{n}}_i) = \begin{pmatrix} \dfrac{\partial F_1(\mathbf{g}^{\mathrm{f}}_t)}{\partial f_{1,t}} & \cdots & \dfrac{\partial F_1(\mathbf{g}^{\mathrm{f}}_t)}{\partial m_{4,t}} \\ \vdots & \vdots & \vdots \\ \dfrac{\partial M_4(\mathbf{g}^{\mathrm{m}}_t)}{\partial f_{1,t}} & \cdots & \dfrac{\partial M_4(\mathbf{g}^{\mathrm{m}}_t)}{\partial m_{4,t}} \end{pmatrix}_{\mathbf{n}_t = \hat{\mathbf{n}}_i} \tag{B-26}$$

is greater than unity ($\lambda(\hat{\mathbf{n}}_i) > 1$). Therefore all genotypes can be invaded when $\lambda(\mathbf{n}_i) > 1$ for all $i \in \{1,2,3,4\}$, which is the condition for selection to be balancing at a minimum of one locus. Plugging eq. (1) into eqs. (B-24)-(B-25), eqs. (B-24)-(B-25) into eqs. (B-22)-(B-23), and then eqs. (B-22)-(B-23) into eq. (B-26) and calculating the relevant eigenvalues we can derive the invasion conditions for all four genotypes. The resulting expressions are typically unsightly and thus not easily interpretable and so are plotted for different numerical values in Supplementary Fig. 1 (bottom row, we interpret these results in the next section, Appendix B.2.3).

Invadability of all genotypes is a sufficient condition for balancing selection to happen at least at one of the two loci. But it is not sufficient to know whether polymorphism will be maintained at both loci simultaneously. To investigate whether balancing selection occurred at one or two loci, we iterated numerically the recursions eqs. (B-22)-(B-23) and recorded how many loci were still polymorphic after 10^5 generations (which was sufficient time for equilibrium polymorphic frequencies to be reached). We did this for a wide range of parameter values within $s_{\mathrm{m}} \in [0,1]$, $b \in [0,2]$ and $\alpha \in [0,1]$ where $s_{\mathrm{f}} = \alpha s_{\mathrm{m}}$, and with initial starting genotype frequencies of $m_1 = f_1 = 0.2499, m_2 = f_2 = 0.2499, m_3 = f_3 = 0.2501, m_4 = f_4 = 0.2501$. If the minor allele frequency at a locus exceeded 10^{-3}, then this locus was considered to be polymorphic and under balancing selection.

B.2.3 Results

Analysis of the two-locus model reveals that polymorphism may be maintained at both loci, at only one locus, or at neither, depending on the shape of fecundity curves (b) and the strength of selection in each sex ($s_{\mathrm{m}}, s_{\mathrm{f}}$).

In line with the results from our continuum-of-alleles approach, polymorphism is maintained across both loci (Supplementary Fig. 1 bottom row panels, black regions) under the conditions that fecundity curves are accelerating ($b > 1$) and selection is strong and of similar strength in both sexes ($s_\mathrm{m} \sim s_\mathrm{f} \gg 0$).

Meanwhile, balancing selection at just one locus requires that fecundity curves are diminishing ($b < 1$) and that selection strength is moderately different between the sexes ($s_\mathrm{m} \neq s_\mathrm{f}$, Supplementary Fig. 1 bottom row panels, gray regions). Here, the allele favouring the more strongly selected sex becomes fixed at one locus (A_1 or A_2 when $s_\mathrm{f} > s_\mathrm{m}$, and a_1 or a_2 when $s_\mathrm{m} > s_\mathrm{f}$) and both alleles persist at the other. In this case, that is, given fixation at one locus, we can use eqs. (B-24)-(B-25) to find the equilibrium allele frequency at the remaining polymorphic locus (i.e. by finding equilibrium frequencies of the two segregating haploid genotypes), as well as the level of heterozygosity this creates. The equilibrium frequency, p_k^*, of the female-beneficial allele A_k at locus k when $s_\mathrm{m} > s_\mathrm{f}$ is

$$p_k^* = \frac{(2^b - 3^b)s_\mathrm{f} + (2^b - 1)s_\mathrm{m}}{(2^b - 2\cdot 3^b) + 4^b)s_\mathrm{f} + (2^b - 2)s_\mathrm{m}} + \mathcal{O}(\epsilon^2) \tag{B-27}$$

(i.e. the frequency of A_1 in a population fixed for a_2, or the frequency of A_2 in a population fixed for a_1, where $s_\mathrm{m} \sim \mathcal{O}(\epsilon)$, $s_\mathrm{f} \sim \mathcal{O}(\epsilon)$, Appendix Fig. 1A), and when $s_\mathrm{m} < s_\mathrm{f}$, the equilibrium frequency, $q_k^* = 1 - p_k^*$, of the male-beneficial allele a_k at locus k is

$$q_k^* = \frac{(2^b - 1)s_\mathrm{f} + (2^b - 3^b)s_\mathrm{m}}{(2^b - 2)s_\mathrm{f} + (2^b - 2\cdot 3^b + 4^b)s_\mathrm{m}} + \mathcal{O}(\epsilon^2) \tag{B-28}$$

(i.e. the frequency of a_1 when the population is fixed for A_2, and a_2 when the population is fixed for A_1, Appendix Fig. 1B). From Appendix Fig. 1A-B we see that, at the polymorphic locus $k \in \{1,2\}$, the frequency of the female-beneficial allele A_k decreases (and accordingly, the frequency of the male-beneficial allele a_k a increases) sharply with the strength of selection in males relative to females ($s_\mathrm{m}/s_\mathrm{f}$). Consequently, there is relatively little parameter space where p_k^* and q_k^* have intermediate frequencies (i.e. close to 0.5), and so average heterozygosity across both loci is typically low even when selection is balancing at one locus (Appendix Fig. 1C-D).

Finally, for the remaining combinations of parameters b, s_m and s_f, selection disfavours polymorphism at both loci (Supplementary Fig. 1 bottom row panels, white regions) driving the fixation of one of the four homozygote genotypes ($\mathrm{A}_1\mathrm{A}_1\mathrm{a}_2\mathrm{a}_2$, $\mathrm{a}_1\mathrm{a}_1\mathrm{A}_2\mathrm{A}_2$, $\mathrm{a}_1\mathrm{a}_1\mathrm{a}_2\mathrm{a}_2$, or $\mathrm{A}_1\mathrm{A}_1\mathrm{A}_2\mathrm{A}_2$).

In sum, when $L = 2$, the parameter space for sexually antagonistic selection to drive polymorphism at at least one locus is relatively permissive, and is similar to that when $L = 1$. However, the conditions for polymorphism at two loci are restrictive, requiring strong selection. Thus, sexual antagonism has only a limited capacity to increase heterozygosity across both loci.

B.3 Dynamics at many loci

To characterise evolutionary dynamics for a polygenic trait, we ran individual-based simulations of our di-allelic model with many loci. All simulations were conducted using SLiM 4 [7].

Following the lifeycle described in section 2, we consider a diploid population of fixed size comprising 5000 adult males and 5000 adult females with non-overlapping generations. At the beginning of the offspring generation, say $t+1$, 5000 male and 5000 female offspring are created, with the mother of each offspring being sampled from amongst the female adults of the previous generation t, and the fathers being sampled from amongst the male adults. Sampling performed is with replacement from a multinomial distribution where the weighting on each individual is given by their fecundity, which, following eq. (1), is

$$\begin{aligned} w_{\mathrm{m}}(z) &= (1-s_{\mathrm{m}}) + s_{\mathrm{m}}\left(\frac{\theta - z}{2\theta}\right)^{b_{\mathrm{m}}} \\ w_{\mathrm{f}}(z) &= (1-s_{\mathrm{f}}) + s_{\mathrm{f}}\left(\frac{\theta + z}{2\theta}\right)^{b_{\mathrm{f}}}, \end{aligned} \tag{B-29}$$

in males and females, respectively. After sampling, adults are removed from the simulations, juveniles become adults and the new generation begins. Recombination and mutation occurs for each juvenile as outlined in section 2.

Simulations were initiated with equal allele frequencies at all loci ($p_k = 0.5$ for all k, where p_k is frequency of allele A at locus k) and with genotypes at Hardy-Weinberg proportions, and run for 10^5 generations. In a given generation, heterozygosity at locus k was calculated as

$$H = 1 - (1-p_k)^2 - p_k^2 \tag{B-30}$$

and average heterozygosity across loci was calculated as

$$H = 1 - \sum_{k=1}^{L} (1-p_k)^2 - p_k^2. \tag{B-31}$$

To produce Fig. 3A, calculations were performed at each generation and then averaged over the last 10^4 generations of a simulation.

C Extensions

C.1 Differently shaped fecundity landscapes in males and females

Here, we repeat our analyses of the continuum-of-alleles and di-allelic models now allowing for fecundity curves to have different shapes in males and females. Specifically, we now allow for different curvatures in

the two sexes, $b_m \neq b_f$ in Eq. (1).

C.1.1 Continuum-of-alleles model

When fecundity curves have sex-specific shapes, evolutionary dynamics are complicated and so we proceeded with a numerical analysis. That is, we first plugged eq. (A-5) into eq. (A-6) and solved eq. (A-7) numerically with eq. (1) to find singular strategies x^*, whose stability was then determined. In particular, we focused on identifying the conditions under which sexual antagonism leads to a singularity exhibiting diversifying selection (i.e. an evolutionary branching point), as the existence of such a point is necessary for selection to favour polymorphism.

Overall, we find that the criteria for diversifying selection when $b_m \neq b_f$ are in line with our results for $b_m = b_f$, with such selection only arising under restricted conditions (Appendix Fig. 2 top row, green region). First, selection must be strong. Second, diversifying selection requires at least one fecundity curve be accelerating ($b_m > 1$ and/or $b_f > 1$), with conditions being most permissive when one curve is accelerating and the other is at least linear (i.e. $b \geq 1$ in the sex with the least accelerating curve, Appendix Fig. 2 top row). Diversifying selection is possible if one fecundity curve is saturating, but requires the curve in the other sex to be especially accelerating (e.g. if $b_f < 1$, b_m needs to well exceed 1, Appendix Fig. 2 top row left-hand panel). Even stronger sexually antagonistic selection is required when one of the curves is saturating than when both are accelerating (Appendix Fig. 2).

C.1.2 Polygenic model

Following Appendix B.3, we ran simulations of our di-allelic model assuming z has a polygenic basis ($L = 10$). As in the case of the sexes showing the same fecundity curves, we find that conditions for which we observe elevated heterozygosity closely resembles those for diversifying selection in the continuum-of-alleles model (Appendix Fig. 2, compare top and bottom rows), indicating that such selection is required for the maintenance of genetic polymorphism across loci. Furthermore, in line with our previouus results, we also find that heterozygosity is greatest where both curves are accelerating and selection is very strong ($b_m > 1$, $b_f > 1$, $s_m = s_f \sim 1$, Appendix Fig. 2, bottom righ-hand panel), as this generates the strongest diversifying selection.

C.2 Loci with different effect sizes

Here, we investigate the case where loci have different phenotypic effects in our di-allelic model, i.e. we allow variation in δ_k among the L loci encoding z.

C.2.1 Two locus model

For the case of $L = 2$, we assume that locus 1 has greater effect than locus 2 and set $\delta_2 = \rho\delta_1$ with $0 < \rho < 1$ (and where allelic effects at loci 1 and 2 are given by eq. 3). Using the same notation as in Appendix B.2 (i.e. z_{ij} is the phenotype encoded by the diploid genotype ij where $i \in \{1,2,3,4\}$ and $j \in \{1,2,3,4\}$ are the paternally and paternally inherited haploid genotypes, respectively), we have the following phenotypes

$$\begin{aligned}
z_{11} &= 2\delta(1+\rho) \\
z_{12} &= 2\delta \\
z_{13} &= 2\delta\rho \\
z_{14} &= 0 \\
z_{22} &= 2\delta(1-\rho) \\
z_{24} &= -2\delta\rho \\
z_{33} &= 2\delta(\rho-1) \\
z_{34} &= -2\delta \\
z_{44} &= -2\delta(1+\rho),
\end{aligned} \tag{C-32}$$

with female and male optima of $\theta = 2\delta(1+\rho)$ and $-\theta = -2\delta(1+\rho)$, respectively. After plugging eq. (C-32) into eqs. (B-22)-(B-25) we analyse this model following the same procedure to that explained in Appendix B.2.

We find that the main consequence of varying the ratio of the locus effect sizes (ρ) is that it adjusts the parameter space for single locus polymorphisms when fecundity curves are diminishing ($b < 1$, Appendix Fig. 3A). This is because variation in the phenotypic contributions across loci modulates the phenotypes encoded by intermediate double homozygote genotypes (i.e. the phenotypes encoded by genotypes $A_1A_1a_2a_2$ and $a_1a_1A_2A_2$ diverge from each other and from $z = 0$ when $\rho < 1$). This changes the specific parameters for which double homozygotes will produce high fitness phenotypes, and thus the conditions that will favour a polymorphic remainder locus. By contrast, ρ has relatively little effect on the conditions for maintaining two polymorphic loci, which still requires accelerating fecundity curves and strong selection ($b > 1$, s_m and s_f large and nearly equal, although note the parameter space for two-locus polymorphisms is more permissive when ρ is small, Appendix Fig. 3B-C).

C.2.2 Polygenic model

To run simulations of our polygenic model ($L >> 1$) when alleles have different effect sizes, we used the same procedure as for equal effects (Appendix B.3), but with the effect sizes of individual loci now being drawn from an exponential distribution with mean 1, i.e. $\delta_k \sim \mathrm{Exp}(1)$. The female optimum, which is given by the maximum phenotype, then is $\theta = \sum_1^L 2\delta_k$, and the male optimum, which is given by the minimum phenotype, is $-\theta =$

$\sum_1^L 2\delta_k$.

We find that heterozygosity patterns are similar to the case with equal effect sizes in the sense that average heterozygosity is only greater than neutral when selection is diversifying (i.e. when $b > 1$ and s_m and s_f being similar and large; Appendix Fig. 4 left-most panels, compare top and bottom). In addition, we find that variation at individual loci that persists when selection is stabilising ($b < 1$) due to the lack of homozygous allelic combinations nearer $x^* = 0$ exhibits the same transient behaviour as in the equal effects case (Appendix Fig. 5). Together with the results of section C.2.1, this indicates that variation in effect sizes across loci weakly influences the conditions under which elevated heterozygosity is expected, and only does so when the number of loci is especially small (e.g. $L = 2$) and variation especially large (ρ small).

C.3 Effect of recombination between loci

Here we relax our previous assumption of free recombination, and ran analyses of our two-locus and polygenic di-allelic model with a lower recombination rate between loci ($r \leq 0.5$).

C.3.1 Two locus model

We analysed the two-locus model with linkage using the recursions eq. (B-24)-(B-25), considering both equal and different phenotypic effect sizes (plugging eq. C-32 into eqs. B-22-B-25 with $\rho = 1$ and $\rho < 1$, respectively).

In general, reduced recombination has a limited effect on the maintenance of genetic variation (Appendix Fig. 6). Specifically, when loci had equal phenotypic effects ($\delta_1 = \delta_2 = \delta$), variation maintained by sexual antagonism was generally insensitive to recombination rate, with the exception that limited recombination moderately reduces the strength of selection required for two-locus polymorphisms to arise under accelerating fecundity curves ($b > 1$, Appendix Fig. 6A). An additional effect of recombination arises when loci have different effect sizes, whereby tight linkage can generate two-locus polymorphisms when fecundity curves are diminishing ($b < 1$ and e.g. $r \sim \mathcal{O}(0.001)$, Appendix Fig. 6B). Here, differences in allelic effect sizes mean that no homozygote genotype encodes a high fecundity intermediate phenotype, and the fittest genotypes are instead double heterozygotes. When recombination is weak, this leads to increased genetic variation because double heterozygotes produce almost exclusively A_1a_2 and a_1A_2 gametes that go on to form high fitness offspring, allowing selection to maintain both gametic genotypes and so two polymorphic loci. Such elevated genetic variation owing to tight linkage has been found in previous studies of sex-concordant stabilising selection [14, 15], although this effect breaks down when the number of trait loci increases ($L > 2$, [15]).

C.3.2 Polygenic Model

When L is polygenic, limited recombination also has a weak effect on genetic variation. The conditions for elevated heterozygosity in the presence of genetic linkage are only slightly more permissive than those with free recombination (still requiring $b > 1$, s_{m} and s_{f} similar and large), even when loci have different effect sizes and recombination is extremely weak (Appendix Fig. 4). Notably, in contrast to the $L = 2$ case, elevated heterozygosity is not observed when $b < 1$ for any recombination rate considered, consistent with the notion that the effects of linkage on genetic variation under stabilising selection in two-locus models do not generalise to arbitrary numbers of loci [15]. This is likely because the large variety of allele combinations possible when L is large means a homozygote genotype is typically available that encodes a fit enough phenotype to fix, and so linkage does not generate conditions for multi-locus polymorphisms. Weak recombination, however, drives higher levels of heterozygosity for the parameter values that lead to diversifying selection (Appendix Fig. 4). This is in line with theory on quantitative traits mediating intraspecific competition, where, under strong diversifying selection, population genetic variance, rather than the space maintaining polymorphism, is sensitive to recombination rate [16].

C.4 Other fitness functions

Our results are based on the fecundity functions described in eq. (1) of the main text. Here we investigate whether there exists other functions that can offer more permissive conditions for the maintenance of polymorphism.

C.4.1 The emergence of polymorphism

We first analyse this model under the continuum-of-alleles model, with a single locus evolving through small effect mutations, with the mutant allele having a similar phenotype $x_\bullet$ to the current resident allele, x. Recall eq. (A-5) that the invasion fitness of the mutant allele is

$$W(x_\bullet, x) = \frac{1}{2}\frac{w_{\mathrm{f}}(x_\bullet + x)}{w_{\mathrm{f}}(2x)} + \frac{1}{2}\frac{w_{\mathrm{m}}(x_\bullet + x)}{w_{\mathrm{m}}(2x)}. \tag{C-33}$$

The selection gradient (eq. A-6) is thus generally given by

$$S(x) = \frac{1}{2}\left[\frac{w'_{\mathrm{f}}(2x)}{w_{\mathrm{f}}(2x)} + \frac{w'_{\mathrm{m}}(2x)}{w_{\mathrm{m}}(2x)}\right]. \tag{C-34}$$

This shows that allelic value x^* is singular if

$$\frac{w'_{\mathrm{f}}(2x)}{w_{\mathrm{f}}(2x)} = -\frac{w'_{\mathrm{m}}(2x)}{w_{\mathrm{m}}(2x)}, \tag{C-35}$$

so that the relative fitness gain in one sex is balanced by the relative fitness loss in the other. Convergence stability (eq. A-8) of x^* depends on the sign of:

$$S'(x^*) = \left[\frac{w_{\mathrm{f}}''(2x)}{w_{\mathrm{f}}(2x)} + \frac{w_{\mathrm{m}}''(2x)}{w_{\mathrm{m}}(2x)}\right] - \left\{\left(\frac{w_{\mathrm{f}}'(2x)}{w_{\mathrm{f}}(2x)}\right)^2 + \left(\frac{w_{\mathrm{m}}'(2x)}{w_{\mathrm{m}}(2x)}\right)^2\right\}, \tag{C-36}$$

while the existence of stabilizing vs. diversifying selection depends on (eq. A-9):

$$H(x^*) = \frac{1}{2}\left[\frac{w_{\mathrm{f}}''(2x)}{w_{\mathrm{f}}(2x)} + \frac{w_{\mathrm{m}}''(2x)}{w_{\mathrm{m}}(2x)}\right]. \tag{C-37}$$

For there to be diversifying selection, we must have $S'(x^*) < 0$ and $H(x^*) > 0$, which requires

$$0 < \left[\frac{w_{\mathrm{f}}''(2x)}{w_{\mathrm{f}}(2x)} + \frac{w_{\mathrm{m}}''(2x)}{w_{\mathrm{m}}(2x)}\right] < \left\{\left(\frac{w_{\mathrm{f}}'(2x)}{w_{\mathrm{f}}(2x)}\right)^2 + \left(\frac{w_{\mathrm{m}}'(2x)}{w_{\mathrm{m}}(2x)}\right)^2\right\} \tag{C-38}$$

The right-hand term in curly braces represents the strength of selection squared in both sexes and so is negligible when selection is weak. Thus, whatever the fecundity functions $w_{\mathrm{m}}(z)$ and $w_{\mathrm{f}}(z)$, selection can never be diversifying and polymorphism can never emerge from gradual evolution when variation in male and female fecundity ($w_{\mathrm{m}}(z)$ and $w_{\mathrm{f}}(z)$) is small. Strong selection can, however, allow for diversifying selection, but only when the fitness surfaces are positively curved, on average across the sexes (first condition), but not so curved that the second condition fails. These results are consistent with those derived in section A.4.1 using the specific fitness functions eq. (1).

C.4.2 The maintenance of polymorphism

We next examine when a polymorphic equilibrium at a locus with two alleles, say x_1 and x_2, is stable to the invasion of a third allele (i.e. is an uninvadable coalition). In general, this requires that we track the frequencies of the two resident alleles in male and female adults separately (as in eq. A-1) and conduct a full stability analysis of the recursions. When selection is weak (in the sense that variation in $w_{\mathrm{m}}(z)$ and $w_{\mathrm{f}}(z)$ is small), however, the allele frequencies are approximately equal in the two sexes. This considerably simplifies analysis and we endorse this assumption throughout this section.

We focus our attention to functions that are symmetric across the sexes (about $z = 0$), which should be the most conducive to polymorphism. Specifically, we set

$$\begin{aligned} w_{\mathrm{m}}(z) &= \phi(-z) \\ w_{\mathrm{f}}(z) &= \phi(z) \end{aligned} \tag{C-39}$$

where $\phi : \mathbb{R} \to \mathbb{R}_{\geq 0}$ is the fecundity function in females. Before considering a polymorphism, we note that a singular trait valued x^* is such that

$$\phi'(2x^*) = \phi'(-2x^*), \tag{C-40}$$

according to eq. (C-35) with eq. (C-39) under weak selection. Hence

$$x^* = 0, \tag{C-41}$$

is always a singular strategy, as expected given that the symmetry of the male and female fecundity curves about $z = 0$. Convergence stability and uninvadability of x^*, meanwhile, are determined by

$$\begin{aligned} S'(x^*) &= \phi''(2x^*) + \phi''(-2x^*) \\ H(x^*) &= \frac{1}{2}\left(\phi''(2x^*) + \phi''(-2x^*)\right), \end{aligned} \tag{C-42}$$

respectively.

Given the symmetry of the fecundity functions (eq. C-39), we expect that two alleles x_1 and x_2 must be equally distant from zero to be part of a stable coalition. So we can set

$$\begin{aligned} x_1 &= -x \\ x_2 &= x, \end{aligned} \tag{C-43}$$

where $x > 0$. Reciprocal invasion of x_1 and x_2 requires that $W(x_1, x_2) > 1$ and $W(x_2, x_1) > 1$, which using from eqs. (C-33) and (C-43) is equivalent to,

$$\phi(0) > \frac{\phi(-2x) + \phi(2x)}{2}. \tag{C-44}$$

This can be seen as the requirement of dominance reversal as it says that the heterozygote (expressing 0) must have greater fecundity than the average of the two homozygotes (expressing $2x$ and $-2x$) in both sexes.

To determine whether a polymorphism consisting of x_1 and x_2 is an uninvadable coalition under the continuum of alleles model, we need to first characterize the invasion fitness $W(x_\bullet, (x_1, x_2))$ of a mutant $x_\bullet$ in a resident population that is polymorphic and at equilibrium (i.e. where the frequencies of x_1 and x_2 have converged to their equilibrium). Because selection is weak and the model shows perfect symmetry among males and females, the equilibrium frequency of each resident allele $x_1 = -x$ and $x_2 = x$ is simply $1/2$ in both males and females. It is straightforward to show that in this case, the invasion fitness of a third allele for the symmetric model (eq. C-39) is given by

$$W(x_\bullet, (-x, x)) = 1 + \frac{1}{4}\Big(\phi(x_\bullet + x) + \phi(x_\bullet - x) + \phi(-x_\bullet - x) + \phi(-x_\bullet + x) - 2\phi(0) - \phi(2x) - \phi(-2x)\Big) + \text{HOT} \tag{C-45}$$

where HOT denotes higher under terms of selection. Directional selection on each allelic value is given by

$$\begin{aligned} S_1(-x, x) &= \left.\frac{\partial W(x_\bullet, (-x, x))}{\partial x_\bullet}\right|_{x_\bullet = -x} \\ S_2(-x, x) &= \left.\frac{\partial W(x_\bullet, (-x, x))}{\partial x_\bullet}\right|_{x_\bullet = x}, \end{aligned} \tag{C-46}$$

respectively. A singular coalition $(-x^*, x^*)$ is defined such that

$$S_1(-x^*, x^*) = S_2(-x^*, x^*) = 0. \tag{C-47}$$

Substituting eq. (C-45) into eq. (C-46), we find that eq. (C-47) requires that

$$\phi'(2x^*) = \phi'(-2x^*), \tag{C-48}$$

i.e. that rises in fecundity in one sex are exactly offset by declines in the other near both resident homozygotes. Such a singular coalition will be approached gradually from nearby coalitions through evolution (i.e. is convergence stable), when the leading real part of the eigenvalues of the Jacobian matrix

$$\begin{pmatrix} \dfrac{\partial S_1(x_1, x_2)}{\partial x_1} & \dfrac{\partial S_1(x_1, x_2)}{\partial x_2} \\ \dfrac{\partial S_2(x_1, x_2)}{\partial x_1} & \dfrac{\partial S_2(x_1, x_2)}{\partial x_2} \end{pmatrix}_{\substack{x_1=-x^* \\ x_2=x^*}}, \tag{C-49}$$

is negative. We find that this is equivalent to

$$\begin{aligned} &\phi''(-2x^*) + \phi''(2x^*) < 0 \\ &2\phi''(0) + \phi''(-2x^*) + \phi''(2x^*) < 0. \end{aligned} \tag{C-50}$$

Note that it is possible for a polymorphic coalition to be stable under weak selection, even though we do not expect evolutionary branching from the singular state at $x^* = 0$. This requires, however, that the fecundity curves be sufficiently negatively curved to satisfy eq. (C-50) and yet also have equal slopes on the fitness surface at both homozygous phenotypes so that eq. (C-48) holds (see Appendix Fig. 7 for an example).

Uninvadability of this coalition with respect to additional alleles requires that

$$\begin{aligned} &\left.\frac{\partial^2 W(x_\bullet, (-x, x))}{\partial x_\bullet^2}\right|_{x_\bullet=-x=-x^*} < 0 \\ &\left.\frac{\partial^2 W(x_\bullet, (-x, x))}{\partial x_\bullet^2}\right|_{x_\bullet=x=x^*} < 0. \end{aligned} \tag{C-51}$$

Plugging eq. (C-45) into eq. (C-51), we obtain that

$$2\phi''(0) + \phi''(-2x^*) + \phi''(2x^*) < 0 \tag{C-52}$$

must hold for the local uninvadability of a singular coalition $(-x^*, x^*)$. The fact that the same condition is necessary for convergence stability (eq. C-50) and for stabilizing selection (eq. C-52) indicates that there are no fecundity functions $\phi(z)$ such that another allele emerges from gradual evolution when the population is already dimorphic (i.e. there is no further branching under weak selection).

Comparing Eqs. (C-48), (C-50) and (C-52) with Eqs. (C-40) and (C-42) reveals that if a singular coalition $(-x^*, x^*)$ is convergence stable and thus uninvadable, then so are either $-x^*$ or x^* in a monomorphic state (i.e. if Eqs. C-48, C-50 and C-52 hold, then so do Eqs. C-40 and C-42). This suggest that when a polymorphism that is locally stable exists, it is not very robust to perturbations as any monomorphic state where one of the two allele is lost is also locally stable.

Additionally, it is relatively straightforward for the strategy $x^* = 0$ (eq. C-41) to invade a stable coalition. Setting $x_\bullet = 0$ into eq. (C-45) and re-arranging, we obtain that this allele will invade a stable coalition when

$$\underbrace{\phi(0) - \frac{\phi(-2x^*) + \phi(2x^*)}{2}}_{>0 \text{ from eq. (C-44)}} - 2\left[\phi(0) - \frac{\phi(-x^*) + \phi(x^*)}{2}\right] > 0, \tag{C-53}$$

which essentially requires that $\phi(z)$ decelerates with z between $-2x^*$ and $2x^*$ (assuming it is monotonic). This can be seen from the fact that

$$\phi(0) - \frac{\phi(-2x^*) + \phi(2x^*)}{2} - 2\left[\phi(0) - \frac{\phi(-x^*) + \phi(x^*)}{2}\right] = -\phi''(0)x^{*2} + \mathcal{O}\left(x^{*4}\right). \tag{C-54}$$

Hence, $\phi''(0) < 0$ favours the invasion of an allele coding for zero in a dimorphic population. In addition, $\phi''(0) < 0$ entails that this allele is convergence stable and uninvadable in monomorphic state (see eq. C-42).

C.4.3 Multiple loci

The above shows there exists fecundity functions $\phi(z)$ such that the population may switch from being monomorphic to polymorphic but that this requires either a polymorphism to exist initially or large step mutations. Where the trait is encoded by multiple loci, such large steps are much less likely as each locus contributes less variation. It is therefore more likely for the population to become monomorphic and remain so even when fecundity functions allow for the existence of stable coalitions.

We explored this with individual-based simulations. Specifically, we considered a version of our di-allelic model where z is encoded by $L = 10$ loci. We use fecundity functions that lead to stable dimorphism in the continuum-of-allele model (see Appendix Fig. 7). We initialise the population with two alleles $-x$ and x present at each locus. We assume that there is initially full linkage disequilibrium, with all alleles of the same sign fully linked on the same homologous copy of a non-recombining chromosome (i.e. an individual carries the same allele at the first copy of every locus, and the same allele at the second copy of every locus). At the beginning of a simulation, chromosomes were allocated as being positive (carrying all x) or negative (carrying all $-x$) with equal probability, so that simulations start with two segregating haplotypes at approximately equal frequency with total phenotypic contributions $10x$ and $-10x$ (as we assume $L = 10$). We initially assumed there was no recombination between loci and no new mutations ($r = 0$, $\mu = 0$). After $10'000$ generations, we allowed recombination to occur ($r > 0$), so that alleles could become shuffled between chromosomes. We recorded av-

erage heterozygosity across loci through time (eq. B-31 where p_k is the frequency of allele encoding x at locus $k \in \{1,\dots,10\}$). The results of simulations with $r = 0.5$, $r = 0.05$, and $r = 0.005$ are shown in Appendix Fig. 8 (with fecundity functions as in Appendix Fig. 7 and $x = 0.059$ so that the two initial haplotypes, $10x = 0.59$ and $-10x = -0.59$, correspond to the stable allelic coalition at one locus for this scenario).

As expected, heterozygosity is initially high when linkage is complete (Appendix Fig. 8, $r = 0$), as both haplotypes are stably maintained at equal frequency by selection. However, once recombination occurs (Appendix Fig. 8, $r > 0$), heterozygosity rapidly decays as the shuffling of alleles reduces the divergence between haplotypes and the polymorphism becomes unstable. This continues until eventually a single haplotype encoding a monomorphic equilibrium eq. (C-40) fixes. Thus, while it is possible under certain conditions for a sexually antagonistic polymorphism to be uninvadable by small-effect mutations and so maintained by selection at a single locus, this does not generalise to the maintenance of genetic variation in a polygenic trait.

D Genomic tests for sexually antagonistic loci

In this appendix, we describe the procedures used to characterise genetic variation under sexual antagonism using methods from population genomics (and generate Fig. 4). We applied two approaches to simulated data: (i) we calculated between-sex F_{ST}, a measure of allelic differentiation; and (ii) we calculated the sex-difference in the covariance between within-individual allele frequency and fitness. Calculations were performed on 1000 replicates after a burn-in of 10^5 generations (in order to provide mutation-selection-drift equilibrium levels of variation). We considered the case where the trait is encoded by ten loci, $L = 10$, and where the total population size is $N = 10'000$ (consisting of $5'000$ females and $5'000$ males).

D.1 Allelic differentiation

We computed between-sex allelic differentiation at each locus $k \in \{1,\dots,10\}$ when polymorphic as

$$F_{\mathrm{ST},k} = \frac{(\nu_{k,\mathrm{f}} - \nu_{k,\mathrm{m}})^2}{4\nu_k(1-\nu_k)}, \tag{D-55}$$

[17, 18] where

$$\nu_{k,u} = \frac{1}{N}\sum_{i=1}^{N} \nu_{k,u,i}, \tag{D-56}$$

where $\nu_{k,u,i} \in \{0, 0.5, 1\}$ is the within-individual frequency of allele A in the parent of sex $u \in \{\mathrm{f},\mathrm{m}\}$ of recruited offspring $i \in \{1,2,...,N\}$, and $\nu_k = (\nu_{k,\mathrm{m}} + \nu_{k,\mathrm{f}})/2$. In other words, $\nu_{k,\mathrm{f}}$ and $\nu_{k,\mathrm{m}}$ are the frequencies of allele A among successful female and male parents respectively, weighted by the number of recruited offspring these parents produced. Eq. (D-55) thus gives a measure of differentiation owing to fecundity selection [19].

We calculated $F_{\mathrm{ST},k}$ in generation 10^5 for each locus $k \in \{1,\dots,10\}$ that was polymorphic with a minor allele

frequency greater that 0.05 and for each replicate simulation. We then pooled all $F_{\mathrm{ST},k}$ values across loci and across simulation replicates, and then sampled 1000 values at random for each treatment, which were used to plot Fig. 4A (this sampling ensured the same number of data points for each treatment). For control, this procedure was then repeated but with the sex of each individual randomly assigned (so that the variable u in each $v_{k,u,i}$ is a Bernoulli distributed random variable with $u = \mathrm{f}$ with probability $1/2$ and $u = \mathrm{m}$ otherwise).

D.2 Associations tests

We also computed the difference in the linear regression slope of reproductive success on the frequency of allele A, separately in males and females. In generation 10^5, for each individual $i \in \{1,\ldots,5000\}$ of sex $u \in \{\mathrm{f},\mathrm{m}\}$, we measured the number $\omega_{u,i}$ of offspring this individual produced and the frequency $p_{k,u,i} \in \{0, 0.5, 1\}$ of allele A it carries at each locus $k \in \{1,\ldots,10\}$. For each sex u and each locus k that is polymorphic with minor allele frequency greater than 0.05, we then fitted a Generalised Linear Model with Poisson error distribution, with reproductive success $\omega_{u,i}$ as a response variable and allele frequency $p_{k,u,i}$ as a fixed effect, to estimate the regression slope $\beta_{k,u}$. Finally, we calculated the absolute between-sex difference in the regression slopes $\Delta\beta_k = |\beta_{k,\mathrm{m}} - \beta_{k,\mathrm{f}}|$.

As with between-sex F_{ST}, we pooled all $\Delta\beta_k$ values across loci and replicates, and then sampled 1000 values at random for each treatment, which were used to plot Fig. 4B (this sampling ensured the same number of data points for each treatment). For control, this procedure was then repeated but with the sex of each individual randomly assigned (so that the variable u in each $v_{k,u,i}$ is a Bernoulli distributed random variable with $u = \mathrm{f}$ with probability $1/2$ and $u = \mathrm{m}$ otherwise).

Appendix Figures

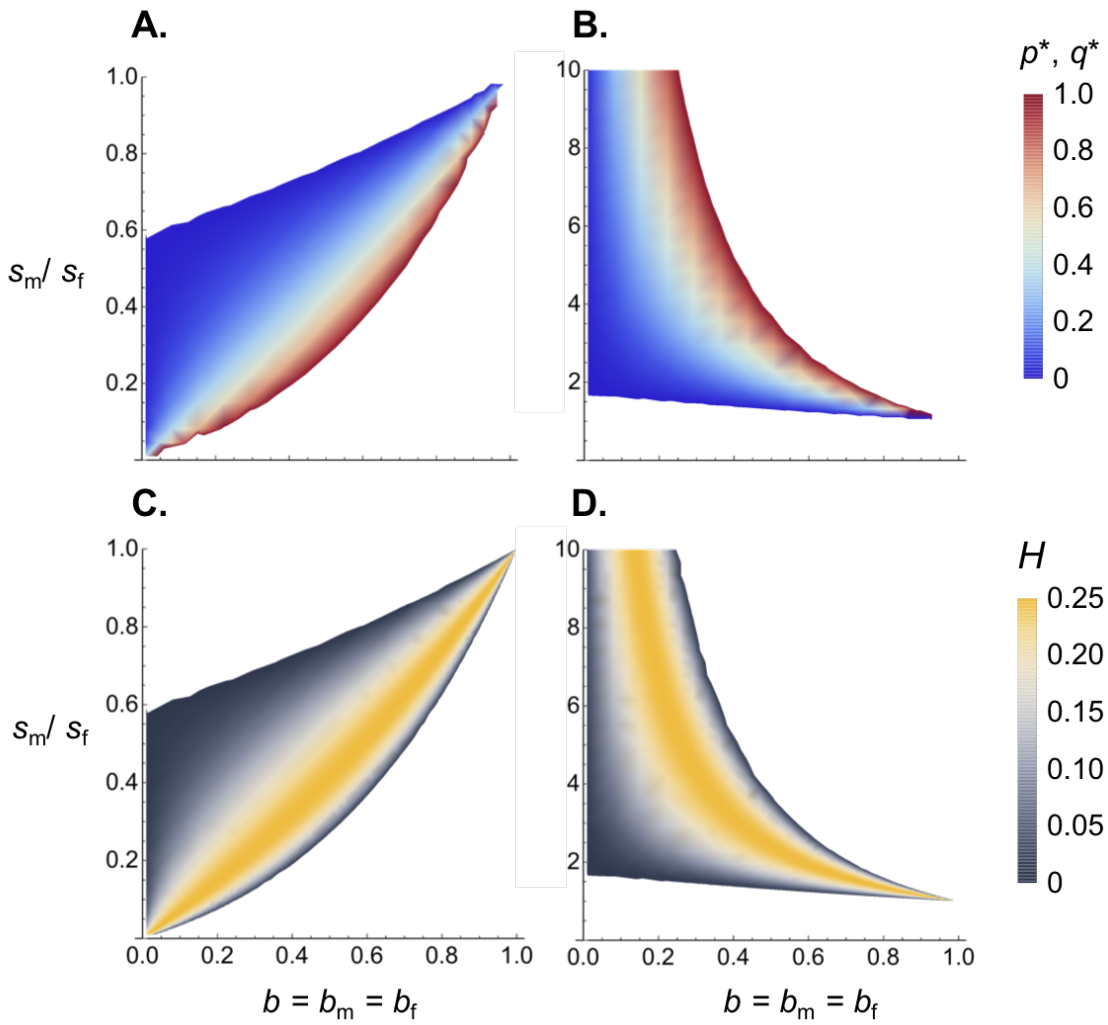

Appendix Figure 1: Genetic variation when one locus is polymorphic in the two-locus model ($L = 2$)**.** Panels **A**-**B** show equilibrium frequencies of allele A_1 (p_1^* in Panel A, eq. B-27) and allele a_1 ($q_1^* = 1 - p_1^*$ in Panel B, eq. B-28) at locus 1 when z is encoded by two di-allelic loci, given that the second locus is fixed for the opposing allele, as a function of the shape of fecundity curves (b) and strength of selection in males relative to females (s_m / s_f). Panels **C**-**D** show average heterozygosity across both loci when one locus is fixed and other at a polymorphic equilibrium ($H = 1 - \sum_{k=1}^{2}(1 - p_k)^2 - p_k^2$, where $p_1 = p_1^*$ and $p_2 = 0$). Other parameters: $s_m = 0.1, \delta = 1$.

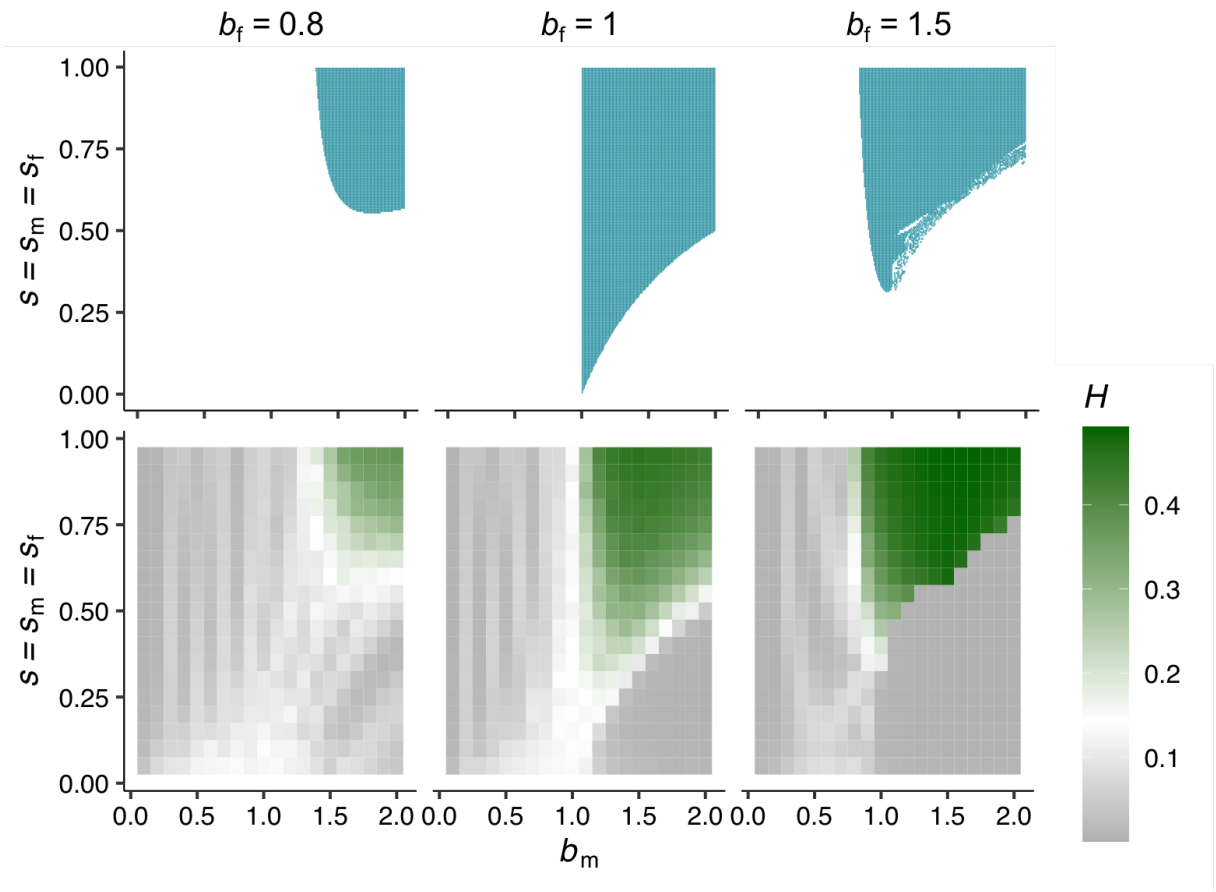

Appendix Figure 2: Conditions for elevated genetic variation when the curvature of the fecundity curves is allowed to differ between the sexes. Top row panels show the conditions for diversifying selection (green regions) in the continuum-of-alleles model depending on the fecundity curve in each sex (b_m, b_f and the strength of selection $s = s_m = s_f$). Bottom row panels show average heterozygosity from polygenic simulations of 10 diallelic loci. Section C.1 for details. Other parameters used: $\delta = 1, \mu = 10^{-5}$.

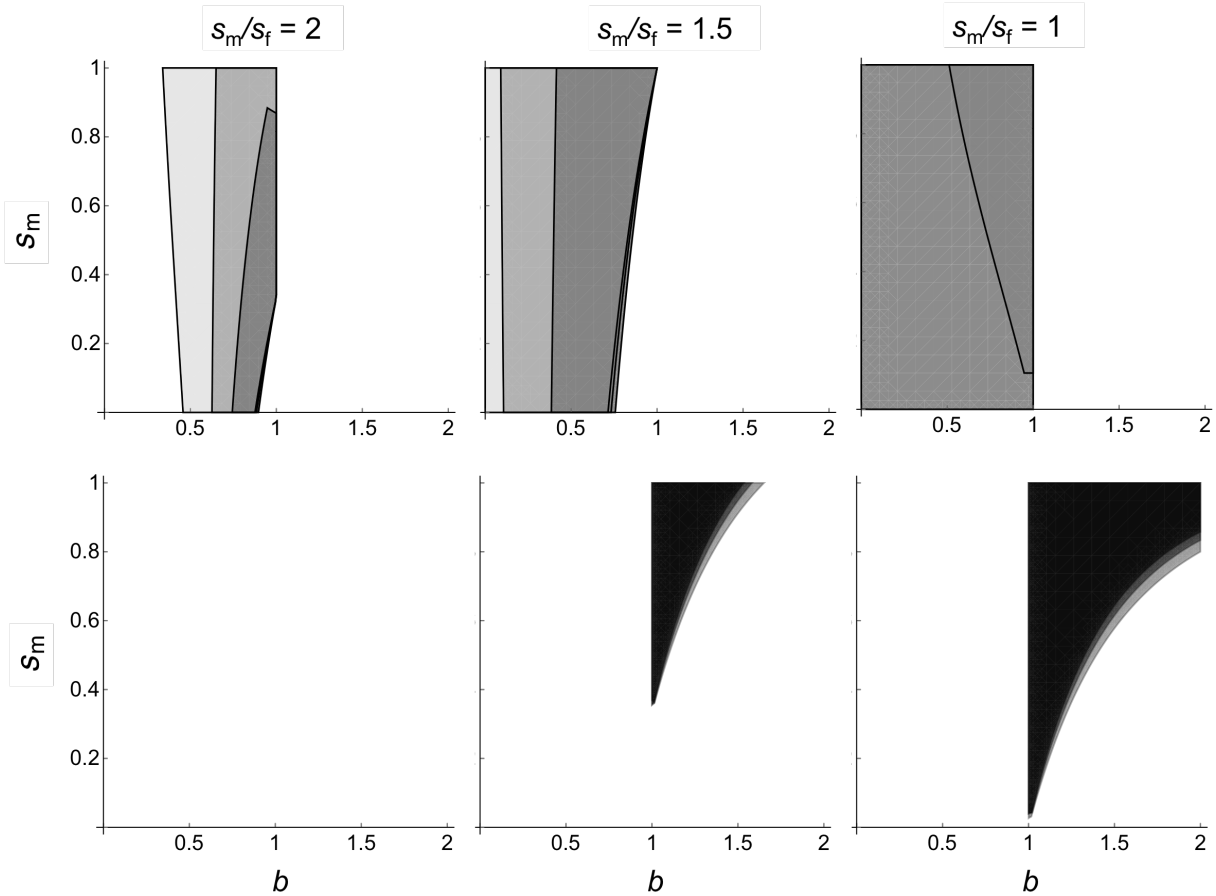

Appendix Figure 3: Conditions for polymorphism in a two-locus trait ($L = 2$) allowing for unequal phenotypic effects. Panels show parameter conditions for one-locus (top row panels) and two-locus (bottom row panels) polymorphisms to be maintained when $L = 2$ and fixed allelic effects. Panels show polymorphism space as a function of equal selection and similarly shaped fecundity landscapes across the sexes ($s = s_m = s_f$ and $b = b_m = b_f$). In all panels, darkest regions show the case of equal effects at both loci ($\delta_1 = \delta_2 = \delta$) and lighter regions show cases of unequal effects ($\delta_2 = \rho\delta_1$), where medium shade shows represents $\rho = 0.5$ and the lightest shade represents $\rho = 0.1$. Other parameters: $\delta = \delta_1 = 1$.

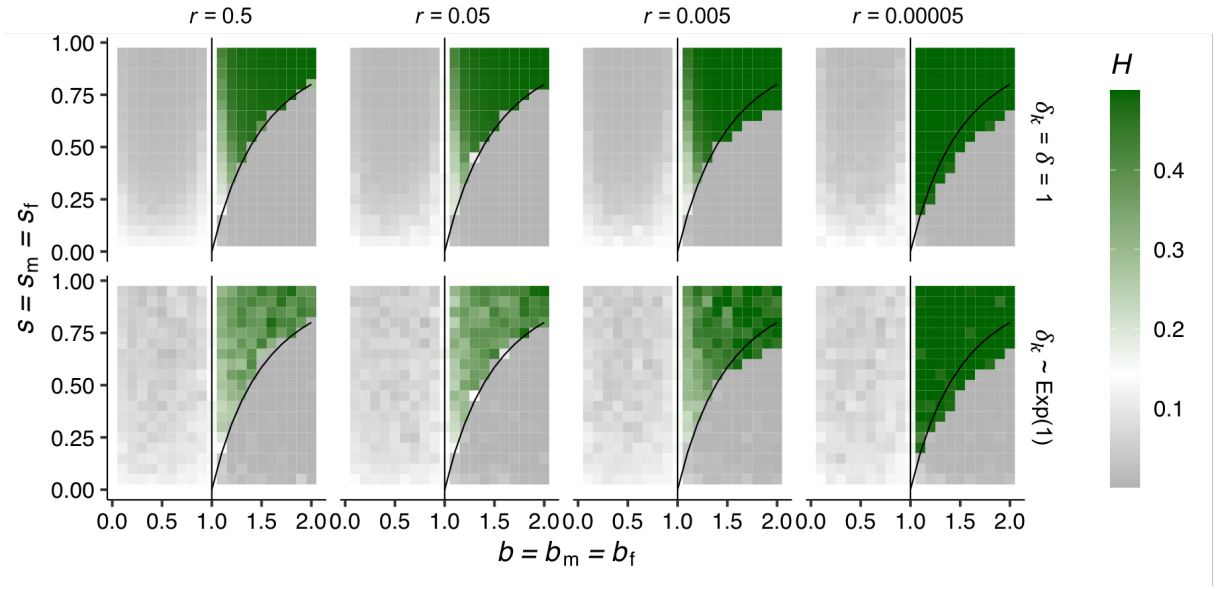

Appendix Figure 4: Average heterozygosity in a polygenic trait for different effect sizes and different strengths of recombination. White, green, and grey squared show average heterozygosity values that are respectively equal, higher, and lower to that expected at a neutral locus at mutation-drift balance. In all panels, $L = 10$. Black lines show the conditions for diversifying selection calculated in the continuum-of-alleles model (eq. A-14). Panels in the top row show results when all alleles have equal effect size ($\delta_k = \delta$ for all $k \in \{1, \ldots 10\}$), while the bottom row allows for unequal effects (where δ_k is drawn from an exponential distribution with mean δ). Columns show results for different strengths of genetic linkage between loci, r. See Appendix B.3 for simulation details.

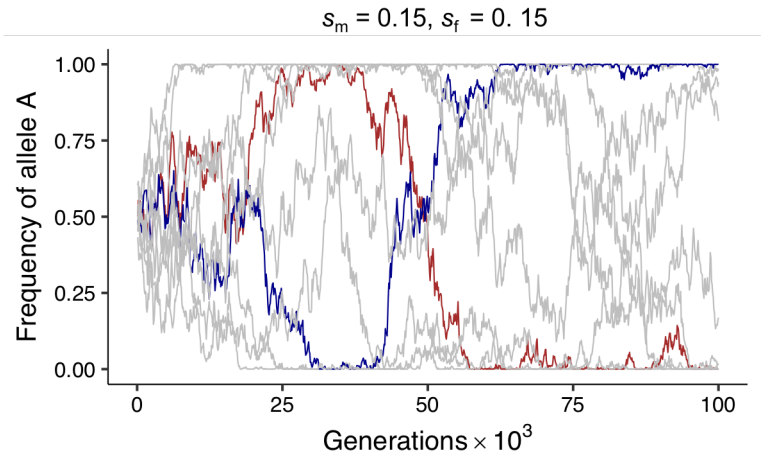

Appendix Figure 5: Allele frequencies through time under stabilising selection with different effect sizes. Curves show frequency of the female-beneficial allele A_k at each locus k through time in a polygenic simulation. Coloured curves show an example of two loci that show transient genetic polymorphism. Results are from simulations with $L = 10$ di-allelic loci, where the effect size δ_k is drawn from an exponential distribution with mean $\delta = 1$. Appendix C.2 for details. Other parameters used: $b = 0.5, \mu = 10^{-5}$.

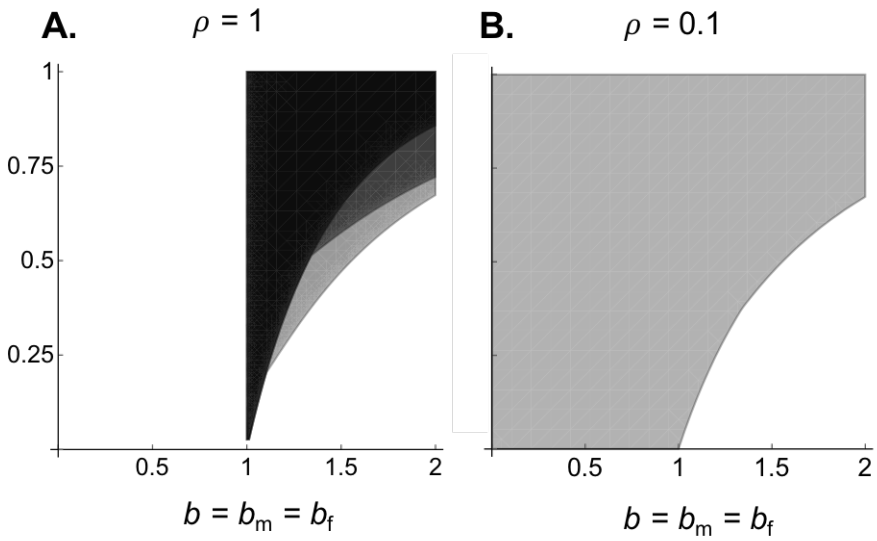

Appendix Figure 6: Polymorphism conditions when $L = 2$ allowing for genetic linkage. Panels show conditions for polymorphism to be maintained at both loci of a two-locus trait ($L = 2$) for the case of equal selection and similarly shaped fecundity landscapes across the sexes ($s = s_m = s_f$ and $b = b_m = b_f$). Panel **A** shows conditions for equal effects across loci ($\delta = \delta_1 = \delta_2$) and Panel **B** shows an example of unequal effects ($\rho = 0.1$ where $\delta_2 = \rho\delta_1$). Different shaded regions correspond to different rates of recombination between loci, black to $r = 0.5$, grey to $r = 0.05$, and light grey to $r = 0.005$. Other parameters: $\delta = \delta_1 = 1$

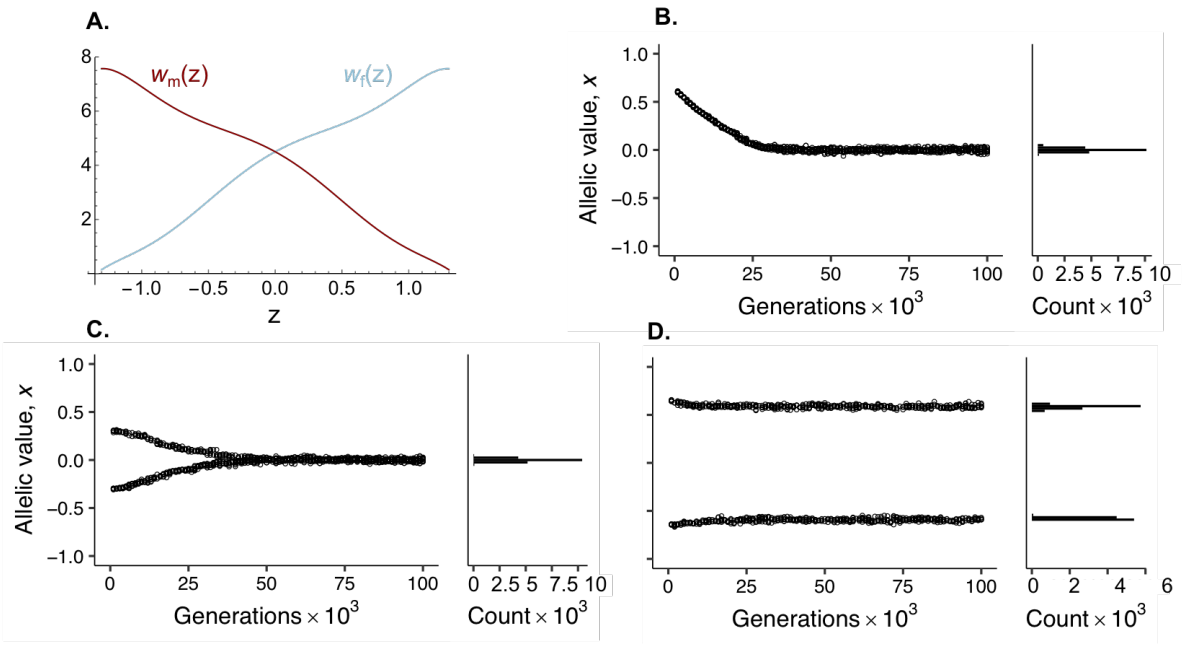

Appendix Figure 7: Continuum-of-allele model with alternative fitness functions. Panel **A** shows the male and female fecundity functions $w_m(z) = \alpha_0 - \alpha_1 z + \alpha_2 z^2 - \alpha_3 z^3 + \alpha_4 z^4 - \alpha_5 z^5 + \alpha_6 z^6$ (red) and $w_f(z) = \alpha_0 + \alpha_1 z + \alpha_2 z^2 + \alpha_3 z^3 + \alpha_4 z^4 + \alpha_5 z^5 + \alpha_6 z^6$ (blue) with $\alpha_0 = 4.5, \alpha_1 = 2.7, \alpha_2 = -2.1, \alpha_3 = 0.6, \alpha_4 = 2.2, \alpha_5 = -0.3, \alpha_6 = -0.7$, which satisfy the criterion (C-50) when selection is weak. For these functions, our mathematical analysis in Appendix C.4.1 indicates there is a stable monomorphic equilibrium at $x^* = 0$ and a stable dimorphic equilibrium at $(-x^*, x^*) = (-0.59, 0.59)$ (note that variation in $w_m(z)$ and $w_f(z)$ as given here is large; we checked through a numerical analysis that these functions entailed the existence of an uninvadable stable coalition at $(-x^*, x^*) = (-0.59, 0.59)$ under strong selection, which was also checked with simulations as shown in Panels B-D). Panels **B**-**D** show simulation results from the continuum-of-alleles model (see Appendix A.5 for details) with fecundity curves shown in Panel **A**. In Panel **B**, simulations were initialised with a single allelic value at $x = 0.59$ (so that the population begins in a monomorphic state). Meanwhile, in Panels **C**-**D** populations are initialised with two alleles at equal frequencies: a negative allele $-x$ and a positive allele x (with $x = 0.3$ for Panel **C** and $x = 0.59$ for Panel **D**). In line with our mathematical analysis, we found it was possible to maintain a stable two-allele polymorphism but only if the population was initialised in a dimorphic state with alleles that were sufficiently diverged from each other (i.e. with large enough x).

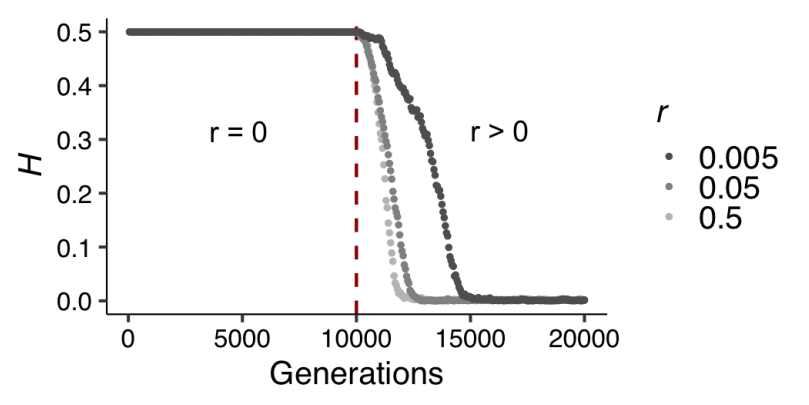

Appendix Figure 8: Heterozygosity across loci in a polygenic trait ($L = 10$) with alternative fitness functions. Plot shows average heterozygosity across loci through time in individual-based simulations of the di-allelic model with fecundity functions given in Appendix Fig. 7A (see legend). Simulations begin with a first phase where there is no recombination among loci ($r = 0$), followed by a second phase beginning at generation 10'000 (dashed red line) where recombination occurs. Different shades of gray refer to different strengths of recombination in the second phase. Appendix C.4.3 for simulation details.

References

[1] Geritz SA, Kisdi É. 2000 Adaptive dynamics in diploid, sexual populations and the evolution of reproductive isolation. *Proceedings of the Royal Society of London. Series B: Biological Sciences* **267**, 1671–1678.

[2] Dercole F, Rinaldi S. 2008 *Analysis of evolutionary processes*. Princeton University Press.

[3] Lande R, Arnold SJ. 1983 The measurement of selection on correlated characters. *Evolution* pp. 1210–1226.

[4] Parker GA, Smith JM. 1990 Optimality theory in evolutionary biology. *Nature* **348**, 27–33.

[5] Geritz SA, Kisdi E, Metz JA et al.. 1998 Evolutionarily singular strategies and the adaptive growth and branching of the evolutionary tree. *Evolutionary ecology* **12**, 35–57.

[6] Rueffler C, Van Dooren TJ, Leimar O, Abrams PA. 2006 Disruptive selection and then what?. *Trends in Ecology & Evolution* **21**, 238–245.

[7] Haller BC, Messer PW. 2019 SLiM 3: Forward genetic simulations beyond the Wright–Fisher model. *Molecular biology and evolution* **36**, 632–637.

[8] Kidwell J, Clegg M, Stewart F, Prout T. 1977 Regions of stable equilibria for models of differential selection in the two sexes under random mating. *Genetics* **85**, 171–183.

[9] Fry JD. 2010 The genomic location of sexually antagonistic variation: some cautionary comments. *Evolution: International Journal of Organic Evolution* **64**, 1510–1516.

[10] Patten MM, Haig D, Ubeda F. 2010 Fitness variation due to sexual antagonism and linkage disequilibrium. *Evolution* **64**, 3638–3642.

[11] Connallon T, Clark AG. 2010 Sex linkage, sex-specific selection, and the role of recombination in the evolution of sexually dimorphic gene expression. *Evolution: International Journal of Organic Evolution* **64**, 3417–3442.

[12] Ubeda F, Haig D, Patten MM. 2011 Stable linkage disequilibrium owing to sexual antagonism. *Proceedings of the Royal Society B: Biological Sciences* **278**, 855–862.

[13] Otto SP. 2019 Evolutionary potential for genomic islands of sexual divergence on recombining sex chromosomes. *New Phytologist* **224**, 1241–1251.

[14] Gavrilets S, Hastings A. 1993 Maintenance of genetic variability under strong stabilizing selection: a two-locus model.. *Genetics* **134**, 377–386.

[15] Bürger R, Gimelfarb A. 1999 Genetic variation maintained in multilocus models of additive quantitative traits under stabilizing selection. *Genetics* **152**, 807–820.

[16] Bürger R, Gimelfarb A. 2004 The effects of intraspecific competition and stabilizing selection on a polygenic trait. *Genetics* **167**, 1425–1443.

[17] Cheng C, Kirkpatrick M. 2016 Sex-specific selection and sex-biased gene expression in humans and flies. *PLoS Genetics* **12**.

[18] Ruzicka F, Dutoit L, Czuppon P, Jordan CY, Li XY, Olito C, Runemark A, Svensson EI, Yazdi HP, Connallon T. 2020 The search for sexually antagonistic genes: Practical insights from studies of local adaptation and statistical genomics. *Evolution letters* **4**, 398–415.

[19] Ruzicka F, Holman L, Connallon T. 2022 Polygenic signals of sex differences in selection in humans from the UK Biobank. *PLoS Biology* **20**, e3001768.